Eastern Hemisphere Tropical Cyclones of 1995

MARK A. LANDER

Water and Energy Research Institute, University of Guam, Mangilao, Guam

MICHAEL D. ANGOVE

Joint Typhoon Warning Center, Nimitz Hill, Guam

(Manuscript received 18 September 1996, in final form 17 March 1997)

ABSTRACT

This paper is designed to be an annual summary of the Eastern Hemisphere tropical cyclones of 1995. The tropical cyclone statistics presented are those of the Joint Typhoon Warning Center, Guam. The text focuses primarily upon the tropical cyclones that occurred in the western North Pacific during 1995; however, since the area of responsibility of the Joint Typhoon Warning Center covers the entire Eastern Hemisphere, brief summaries of the tropical cyclone activity within the north Indian Ocean, south Indian Ocean, and the southwest Pacific are also presented. Overall, 1995 was a relatively quiet year in the Eastern Hemisphere: the 22 tropical cyclones of the Southern Hemisphere were only one shy of the record low of 21, and for the first time since 1988 the number of tropical storms and typhoons in the western North Pacific was below normal. In the western North Pacific, there was a marked shift to the west of the preferred region for the genesis and development of tropical cyclones. This is consistent with the end of persistent large-scale circulation anomalies characteristic of the warm phase of the El Niño–Southern Oscillation (ENSO) and the onset (during 1995) of weak ENSO cold-phase anomalies (i.e., La Niña conditions).

1. Introduction

This summary of the tropical cyclones (TC) of the Eastern Hemisphere during 1995 was compiled from the archives of the Joint Typhoon Warning Center, Guam (hereafter, JTWC). The JTWC was activated on 1 May 1959 as the Fleet Weather Central/Joint Typhoon Warning Center. It is a joint navy–air force activity. Located atop Nimitz Hill, Guam, the JTWC has a forecast area of responsibility (AOR) that extends from the 180° meridian westward to the coast of Africa, in both hemispheres. Seventy percent of the world's tropical cyclones (TC) develop in this AOR. The Naval Pacific Meteorology and Oceanography Command, Pearl Harbor, Hawaii, provides TC warnings for Southern Hemisphere (SH) TCs east of 180°, but these TCs are included in the JTWC SH summary.

Historically, the JTWC has provided a summary of the TCs within its AOR in its Annual Tropical Cyclone Report (ATCR) (e.g., JTWC 1994). The ATCR has a limited distribution, and there have been requests that the JTWC provide an annual summary in *Monthly Weather Review* (*MWR*) similar to the Atlantic and eastern North Pacific TC summaries that the National Hurricane Center (NHC) publishes therein. Thus, for the first time, the JTWC annual TC summary has been adapted for publication in *MWR*, and we hope to continue to provide it.

JTWC warnings and reconnaissance information are made available to all nations in or near the specific ocean basins, as well as to national meteorological centers around the world. The Japan Meteorological Agency (JMA) [the civilian meteorological center designated by the World Meteorological Organization (WMO) to be the regional specialized meteorological center (RSMC) for the issuance of TC warnings in the Western North Pacific (WNP)] uses JTWC's naming convention for tropical storms and typhoons. In addition to the JMA, the JTWC AOR contains numerous local and regional warning centers, including other WMO-designated RSMCs (e.g., Darwin, Fiji, New Delhi, La Réunion, etc.). Outside of the WNP, the JTWC applies numbers to the TCs, but (when available) uses the names given to them by the respective RSMC. Although there is no official collaboration between the JTWC and the RSMCs within its AOR, there is exchange of data, open dissemination of warnings and numerical guidance, and occasionally some personal communication. For more details on the JTWC, its history, its structure, and its organization, see Guard et al. (1992).

Whereas JTWC's main focus is on the TCs of the WNP, the summary of the TCs in this basin is therefore

Corresponding author address: Mark A. Lander, Water and Energy Research Institute, University of Guam, Mangilao, Guam 96911.

TABLE 1. Western North Pacific 1995 tropical cyclone statistics.

Tropical cyclone number	Name	Class[a]	Dates[b]	Maximum 1-min wind (m s^{-1})	Minimum SLP (mb)
1	(01W)	TD	8 Jan	15	1000
2	Chuck	TS	28 Apr–1 May	18	1002
3	Deanna	TS	1–9 Jun	23	991
4	Eli	TS	4–8 Jun	21	994
5	Faye	TY	16–24 Jul	54	938
6	(Unnamed)	TS	26–29 Jul	18	996
7	Gary	TY	29–31 Jul	33	976
8	Helen	TY	7–12 Aug	36	972
9	Irving	TS	17–20 Aug	31	980
10	Janis	TS	21–26 Aug	28	984
11	(11W)	TD	22–23 Aug	13	1002
12	Kent	STY	26 Aug–1 Sep	67	910
13	Lois	TY	26–30 Aug	33	976
14	Mark	TY	30 Aug–2 Sep	49	949
15	Nina	TS	2–7 Sep	23	991
16	(16W)	TD	9–11 Sep	15	1000
17	Oscar	STY	11–18 Sep	72	898
18	Polly	TY	14–21 Sep	46	954
19	Ryan	STY	15–24 Sep	67	910
20	Sibyl	TY	28 Sep–3 Oct	49	949
21	(21W)	TD	28–29 Sep	13	1002
22	(22W)	TD	1–2 Oct	15	1000
23	(23W)	TD	5–6 Oct	13	1002
24	Ted	TY	9–13 Oct	39	958
25	Val	TS	9–14 Oct	23	991
26	Ward	STY	16–22 Oct	72	898
27	Yvette	TY	23–26 Oct	33	976
28	Zack	TY	25 Oct–1 Nov	62	922
29	Angela	STY	25 Oct–6 Nov	80	879
30	Brian	TS	1–4 Nov	26	987
31	Colleen	TS	12–13 Nov	18	996
32/33	(32W/33W)[c]	TD	2–4 Dec	15	1000
34	(34W)	TD	8–11 Dec	15	1000
35	Dan	TS	26–31 Dec	28	984

[a] TD: tropical depression, wind speed less than 17 m s^{-1}. TS: tropical storm, wind speed 17–32 m s^{-1}. TY: typhoon, wind speed 33 m s^{-1} or higher. STY: supertyphoon, subset of the typhoon category with wind speed greater than 66 m s^{-1}.

[b] Dates begin at 0000 UTC and include only the period of warning.

[c] In postanalysis, it was determined that TD 33W was the regenerated TD 32W.

more detailed than are the summaries of TCs in the other basins within the JTWC AOR. An extensive summary of the 1995 TCs in the WNP is found in section 2, which is subdivided into three topics: (a) an overview of the annual TC statistics coupled with a discussion of the large-scale circulation, (b) a recap of the TC activity by month, and (c) short discussions of some selected TCs. A brief summary of the JTWC statistics for the North Indian Ocean (NIO) is found in section 3, and a brief summary of the JTWC statistics for the Southern Hemisphere (SH) is found in section 4. Concluding remarks are found in section 5.

2. Western North Pacific tropical cyclones: January–December 1995

a. Annual statistics and the large-scale circulation

The year of 1995 included five supertyphoons, nine lesser typhoons, 12 tropical storms, and eight tropical depressions (Table 1). The calendar-year total of 34 significant TCs[1] in the WNP was three above the long-term (36-yr) average; however, the year's total of 26 TCs of at least tropical storm intensity was two below the long-term average (Fig. 1). Nineteen ninety-five was the first year since 1988 during which the number of TCs of at least tropical storm intensity was below normal. Likewise, the total of 15 typhoons was below the long-term average of 18—since 1959, 12 years (1969, 1970, 1973–1980, 1983, and 1988) have had 15 or less typhoons. Curiously, most of the years with a low number of typhoons occurred during an 8-yr run from 1973 to 1980.

Twenty-nine of the 34 significant TCs in the WNP

[1] Postanalysis indicated that Tropical Depression 33W was the regeneration of Tropical Depression 32W, and the two best tracks were combined as one.

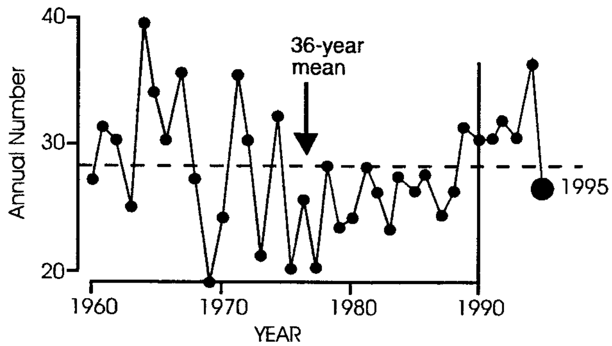

FIG. 1. Tropical cyclones of tropical storm or greater intensity in the western North Pacific (1960–95)

during 1995 originated in the low-level monsoon trough or near-equatorial trough. Three—Typhoon Mark (14W), Tropical Depression 22W, and Tropical Storm Brian (30W)—formed at relatively high latitude in association with cold-core cyclonic vortices in the tropical upper-tropospheric trough (TUTT). Small-sized Tropical Depression 11W formed from a mesoscale convective system that was located to the north of Tropical Storm Janis (10W), and Tropical Storm Colleen (31W) formed in association with a late-season cutoff upper low at higher latitude near the international date line. There were two significant TCs in the WNP during 1995 that originated east of the international dateline—Tropical Depression 01W and Colleen (31W)—however, neither of these TCs was warned on by the Central Pacific Hurricane Center (CPHC) or the NHC before they entered the JTWC's area of responsibility. Historically, about one TC per year named by the CPHC or the NHC moves into the WNP.

With few exceptions, TC formation was confined to the South China Sea (SCS) and the Philippine Sea from May through the end of the year (Fig. 2a). As a consequence, the annual mean genesis location (Fig. 2b) was west of normal—the first such occurrence since 1990. The annual mean genesis location of TCs that form in the WNP is strongly linked to the status of ENSO, and tends to be east of normal during El Niño years and west of normal during La Niña years.

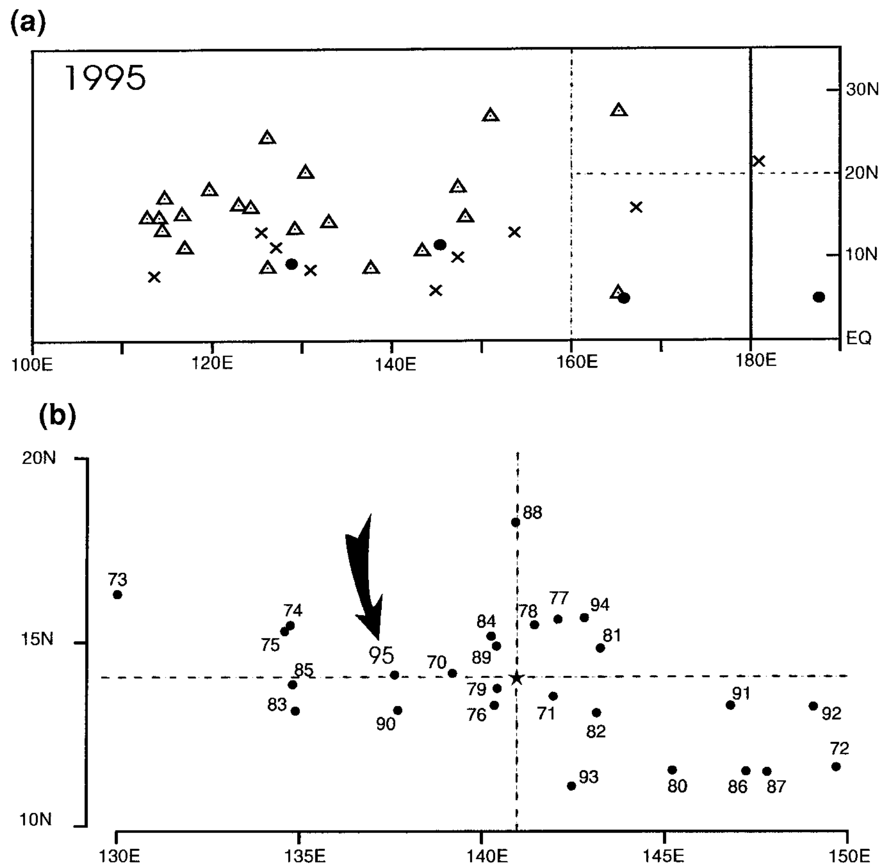

FIG. 2. (a) Point of formation of significant tropical cyclones in 1995 as indicated by the first intensity of 25 kt on the JTWC best track. The symbols indicate: solid dots—1 January–15 July; open triangles—16 July–15 October; and, ×—16 October–31 December. (b) Mean annual genesis location for the period 1970–95 (1995's location is indicated by the arrow). The star lies at the intersection of the 26-yr average latitude and longitude of genesis. For statistical purposes, genesis is defined as the first 25 kt (13 m^{-1}) intensity on the best track.

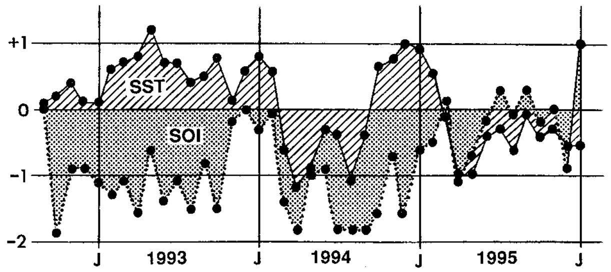

FIG. 3. Anomalies from the monthly mean for eastern equatorial Pacific Ocean sea surface temperature (cross hatched) in degrees Celsius and the Southern Oscillation index (SOI, shaded) for the period 1993–95. [Adapted from Climate Prediction Center (CPC) 1995.]

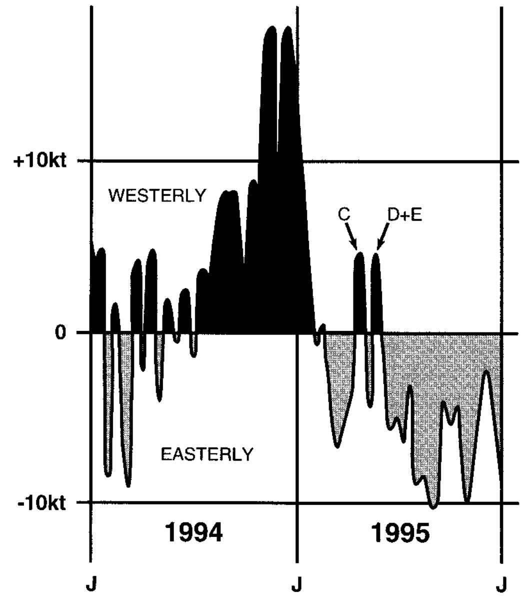

FIG. 4. Time series of the daily low-level wind along the equator at 150°E during 1994 and 1995. Westerly winds are black, easterlies are shaded. The C indicates the time of formation of Chuck (02W), and the D and E indicates the time of formation of Deanna (03W) and Eli (04W). The winds were adapted from the Climate Prediction Center (1995).

Indeed, 1995 saw the end of a prolonged period of the warm phase of ENSO. Large-scale atmospheric and oceanic circulation anomalies indicative of the warm phase of ENSO [e.g., consistently warmer than normal sea surface temperature (SST) over much of the eastern equatorial Pacific (i.e., El Niño conditions), a strongly negative Southern Oscillaticn index (SOI), and a penetration of monsoon westerlies in the WNP far to the east of normal], rapidly returned to near normal, or even reversed during the first half of 1995. By July of 1995, the SST along the equator in the central and eastern Pacific had become colder than normal (Fig. 3), the SOI had risen to near zero (Fig. 3), and low-level easterly wind anomalies replaced westerly wind anomalies in the low latitudes of the WNP (Fig. 4). Based on these Pacific basin SST patterns and the distribution of wind and surface pressure in the Tropics of the Pacific basin, the U.S. Climate Prediction Center (along with other international meteorological centers) declared that the warm phase of ENSO was over. In some respects (e.g., the cooling of the equatorial sea surface, and the anomalously strong low-level easterly winds in the low latitudes of the WNP), the climatic anomalies of the Pacific basin during most of 1995 were consistent with those expected during a cold phase of ENSO, sometimes referred to as La Niña or El Viejo.

During the first few months of 1995, low-level westerly winds still dominated equatorial latitudes of the WNP. By June, however, a weak monsoon trough across Micronesia was replaced by low-level easterlies, and southwesterly winds became restricted to the SCS and within a narrow band south of the mei-yu front (Fig. 5a). Thereafter, the low-level wind of the tropical Pacific became dominated by easterly flow (a hallmark characteristic of La Niña years). As a consequence, the summer monsoon circulation of the WNP was weak—in stark contrast to the very active summer monsoon of 1994. During June, July, and August of 1995, low-level easterly wind flow was unusually persistent in the low latitudes of the WNP (Fig. 6a), and the normal southwest monsoon of the Philippine sea (Fig. 5b) (with its episodic extensions further eastward) was replaced by mean monthly easterly flow. Also, during these months, the axis of the low-level subtropical ridge was displaced approximately 5° equatorward of normal. Corresponding anomalies in the upper troposphere consisted of westerly wind anomalies over the low latitudes of the WNP (Fig. 6b). Low-level easterly anomalies coupled with upper-tropospheric westerly anomalies resulted in strong westerly shear over the deep Tropics of the WNP. This may be related to the large number of weak and poorly defined TCs during much of the year (Fig. 7).

Only two relatively active monsoon episodes were noted during 1995: a reverse-oriented monsoon trough (Lander 1996) (e.g., Fig 5c) formed during mid-September and a large monsoon gyre (Lander 1994a) (e.g., Fig 5d) formed during mid-October. Neither of these events brought exceptionally strong southwesterly monsoon winds into the WNP, but each did briefly shift the southwest monsoon eastward.

The axis of September's reverse-oriented monsoon trough stretched from the SCS eastward across Luzon and the Philippine Sea, and then northeastward to the northeast of Guam. This episode of a reverse-oriented monsoon trough saw the simultaneous development of three TCs along its axis—Oscar (17W), Polly (18W), and Ryan (19W). Polly and Ryan moved on ''S''-shaped tracks: an unusual type of TC track that is almost always associated with reverse orientation of the monsoon trough axis (Lander 1996).

After Oscar, Polly, and Ryan recurved into the midlatitudes during the latter half of September, easterly winds returned to most of the WNP basin. In the mean,

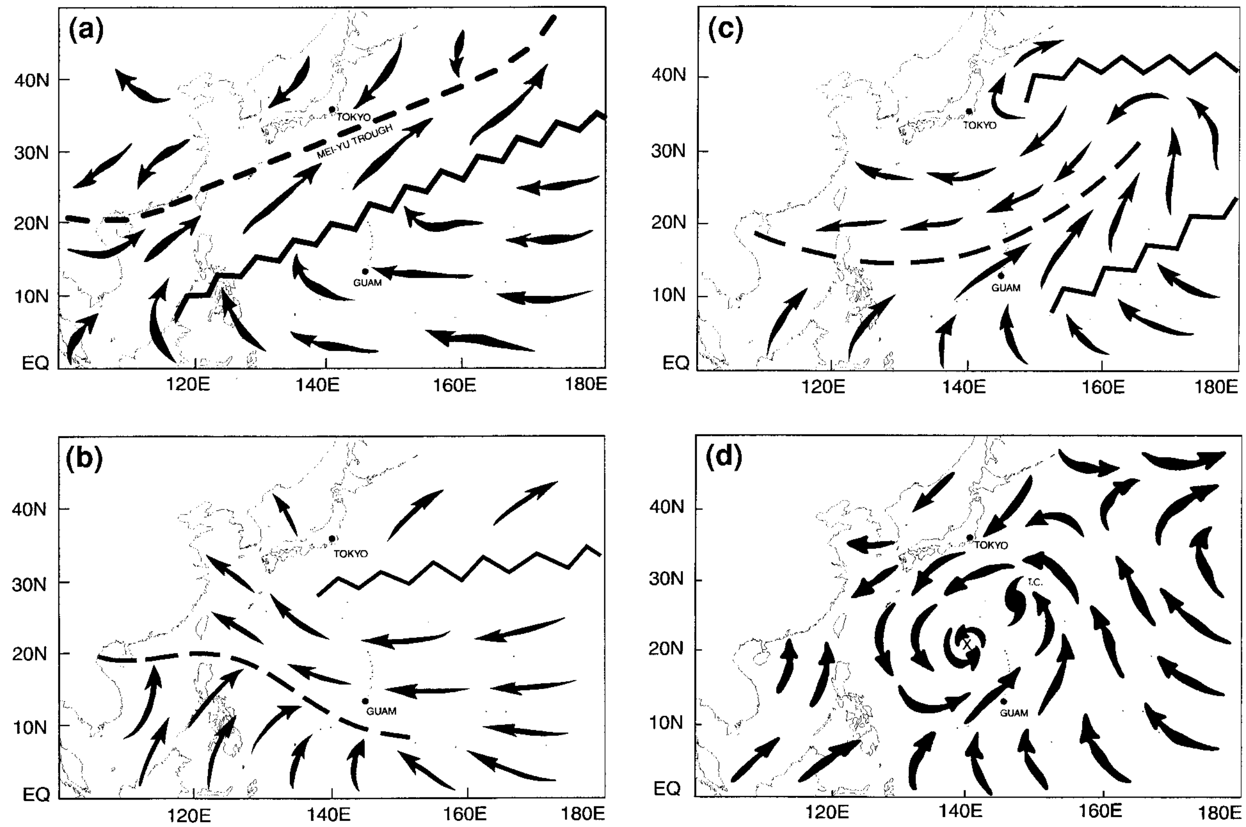

FIG. 5. Patterns of the low-level circulation during the summer in the Tropics of the WNP. (a) Schematic example of the low-level circulation associated with dominant easterly flow in low latitudes and southwesterlies restricted to the South China Sea and to the south of the mei-yu trough. (b) Schematic example of the long-term average. (c) Schematic example of the low-level circulation associated with a reverse-oriented monsoon trough. (d) Schematic example of the low-level circulation associated with a monsoon gyre. Arrows indicate the low-level wind direction. Bold zigzag lines indicate ridge axes, and bold dashed lines indicate trough axes. In (d), "×" indicates gyre center, and a tropical cyclone is shown within the circulation of the gyre.

during October, the axis of the monsoon trough extended across Luzon and into the Philippine Sea to the southwest of Guam. This is where it remained for most of the month with one major exception: during mid-October a large monsoon gyre formed in the Philippine Sea. Tropical Storm Val (25W) interacted with this monsoon gyre. After the monsoon gyre dissipated in the latter half of October, the monsoon trough axis became re-established across the Philippine Sea from Luzon to the southwest of Guam. During the latter half of October, all TCs, except the TUTT-related Brian (30W), formed near, or west, of Guam.

November is normally the month of farthest eastward penetration of monsoonal westerly winds in the WNP. During November 1995, however, the low-level winds at low latitudes and along the equator were easterly from the international date line to the Philippines. Tropical cyclone formation during November was restricted to the SCS and near the Philippines, with the exception of Colleen (31W), which developed from a cutoff low at relatively high latitude near the international date line. Easterly wind anomalies continued during December, and the month's only named TC—Dan (35W)—formed near the Philippines.

In summary, an illustration of all the TC activity in the JTWC AOR during 1995 is provided in Fig. 8. Table 1 lists the significant TCs in the WNP during 1995. Composite best tracks for the WNP TCs are provided for the periods: 1 January–1 September (Fig. 9a), 21 August–14 October (Fig. 9b), and 5 October–31 December (Fig. 9c).

The year that saw the end of prolonged El Niño conditions, 1995, can be described as a year with a weak monsoon, a below average number of typhoons, many weak and poorly defined TCs, and a westward shift of the formation region of TCs in the WNP.

b. WNP monthly activity summary

1) JANUARY

Tropical Depression 01W occurred in January in the near-equatorial trough. January TCs are most properly considered to be late season, born in atmospheric con-

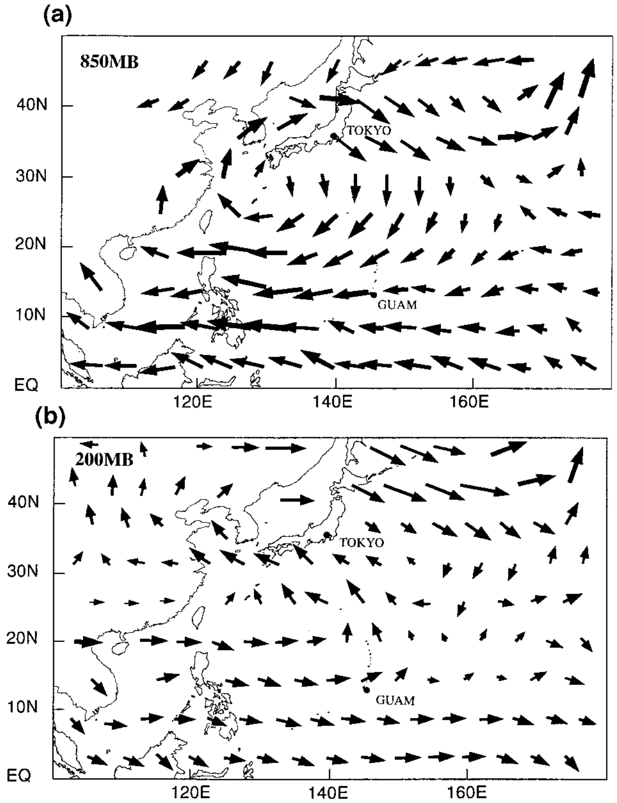

FIG. 6. August wind anomalies: (a) 850 mb and (b) 200 mb. Arrows indicate wind direction and arrow length is proportional to wind speed. In (a) the longest arrows indicate wind anomalies of approximately 5 m s^{-1}. The low-latitude westerly wind anomalies at 200 mb and the low-latitude easterly wind anomalies at 850 mb are both approximately 5 m s^{-1}—the discrepancy of arrow length is due to the fact that the 200-mb arrows are scaled approximately one-third the length of the 850-mb wind arrows. The location of Guam and Tokyo are indicated. [Wind anomalies are adapted from the Climate Prediction Center (1995).]

ditions that evolved during November and December of the previous calendar year.

2) FEBRUARY

The month with the lowest average number of TCs in the WNP is February. In keeping with climatology, there were no significant TCs in the WNP during February 1995.

3) MARCH

Climatology shows a small increase (over February) in the number of TCs in the WNP during March. Tropical cyclones occurring during March are related to the status of ENSO, and during El Niño years there tends to be an increased number of early season (March–June) TCs (Lander 1994b). Consistent with the demise of El Niño conditions during 1995, there were no significant TCs in the WNP during March.

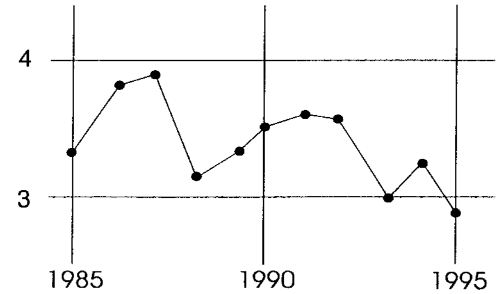

FIG. 7. Average intensity of all tropical cyclones in the WNP for each year from 1985 to 1995. Intensity units are based upon the following categories: 1 =25–44 kt; 2 = 45–63 kt; 3 = 64–80 kt; 4 = 81–95 kt;5 = 96–115 kt; 6 = 116–135 kt; and, 7 = >135 kt. Categories 3–7 are identical to categories 1–5 on the Saffir–Simpson hurricane scale (Simpson 1974).

4) APRIL

One TC—Chuck (02W)—was active during April. The tropical disturbance from which this first named TC of 1995 developed formed in the Marshall Islands at the end of the month. Chuck was a named TC for only two days and peaked at 35 kt (18 m s^{-1}).

5) MAY

During the first week of May, the remnants of Chuck drifted toward the Mariana Islands bringing Guam about one-quarter of its rainfall for the month of May. The tropical disturbances that became Deanna (03W) and Eli (04W) formed in a weak monsoon trough that stretched across Micronesia during late May. They were not named TCs until early June.

6) JUNE

Deanna (03W) was a relatively weak TC that crossed the central Philippines on 2 June. It stalled in the SCS for about two days and then accelerated toward the northeast as it came under the steering influence of strong southwesterly flow to the south of the axis of the mei-yu trough. (The term mei-yu—the Chinese expression for plum rains—has been used to describe the annual recurrence of a persistent zone of disturbed weather in the subtropics of east Asia during spring that usually shifts northward during the months of July and August.) Deanna merged with the mei-yu cloud band as it moved rapidly northeastward through the Ryukyu island chain. Eli (04W), also a weak TC, passed very close to Guam on 4 June. The system turned northward, and dissipated over open water southeast of Japan.

7) JULY

July 1995 was a relatively quiet month in the WNP with only three named TCs active during the month. Forming at midmonth, Faye (05W) was the first TC of 1995 to become a typhoon. Reaching typhoon intensity

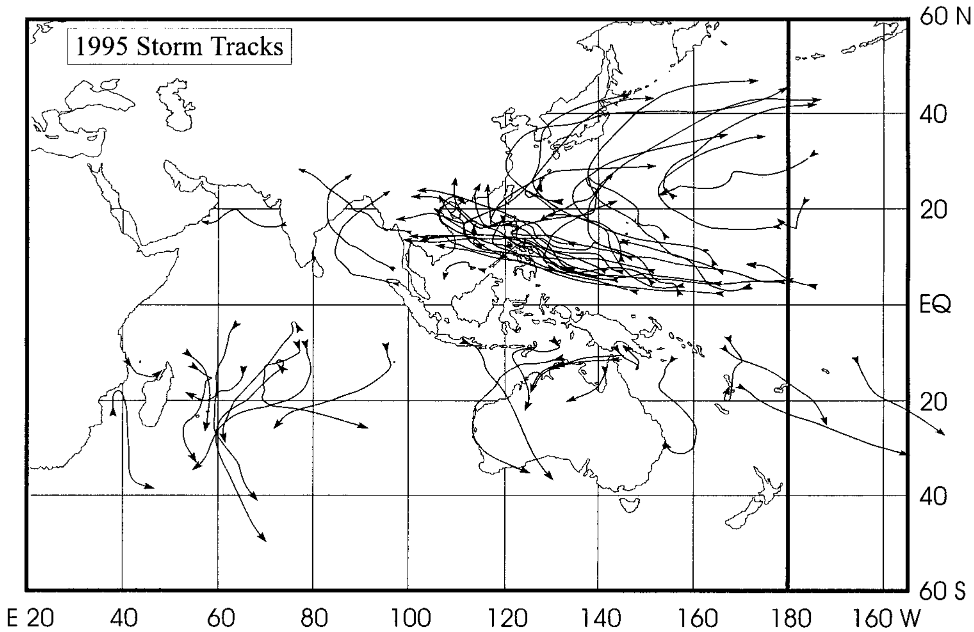

FIG. 8. Composite best tracks of all tropical cyclones warned on by the JTWC during 1995.

on 19 July, Faye tied the record for the latest date for the occurrence of a typhoon in the WNP. Moving on a north-oriented track through the East China Sea, Faye made landfall on the southern coast of Korea, and was one of the most intense TCs to strike the Korean peninsula in many years.

In postanalysis, Tropical Depression 06W (TD 06W) was upgraded to Tropical Storm 06W based upon scatterometer data from the European Space Agency's remote sensing (*ERS-1*) satellite. These data indicated that an area of 35-kt wind speed accompanied TD 06W as it moved northward just off the east coast of Luzon on 28 July. Tropical Storm 06W merged with Tropical Storm Gary (07W) during a time when both of these TCs were embedded within the circulation of a larger monsoon depression, and while both were affected by the island of Luzon.

Gary (07W) merged with Tropical Storm 06W during a time when both of these TCs were embedded within the circulation of a large monsoon depression near the island of Luzon. Forming in the SCS, Gary made landfall in southeastern China very close to the city of Shantou. Based upon ship reports received in the Weekly Tropical Cyclone Summaries compiled by J. Beven of the Tropical Prediction Center, and upon delayed reports of typhoon intensity wind speeds experienced in the city of Shantou, Gary was upgraded from a tropical storm to a typhoon in postanalysis.

8) AUGUST

The pace of TC formation picked up during August with a total of seven significant TCs active during the month. Originating near Guam during the first week of August, the tropical disturbance that became Helen (08W) was slow to develop, taking six days to reach tropical storm intensity. Helen skirted northern Luzon and reached a peak intensity of 70 kt (36 m s^{-1}) just before making landfall east of Hong Kong. Helen was upgraded to typhoon intensity in postanalysis based on data obtained from Hong Kong. A week later, Irving (09W) formed in the SCS. Irving was very small, and isolated in an otherwise relatively cloud-free region over the SCS. It maintained a very small central dense overcast (CDO) under which microwave imagery indicated the presence of an eye.

During the middle of August, a weak monsoon trough extended into the Philippine Sea. Forming in this monsoon trough, Janis (10W) moved northwestward and merged with Tropical Depression 11W (TD 11W). TD 11W formed in association with a TUTT-induced area of convection to the north of Janis. In an unusual case of TC merger, the larger Janis lost much of its deep convection and became less organized as it merged with the smaller TD 11W. Subsequent to the merger, all deep convection was lost, but later regenerated as the system moved northward east of Shanghai. Moving eastward across the Yellow Sea, Janis made landfall in central Korea near Seoul. Heavy rain and winds associated with Janis had a significant impact on South Korea.

As Janis was undergoing recurvature, two TCs formed simultaneously in the monsoon trough: Kent (12W) in the Philippine Sea, and Lois (13W) in the SCS. Kent was the first of five super typhoons to occur in 1995. It rapidly intensified as it approached the Luzon Strait. Basco, Batan Island (WMO 98135), which was

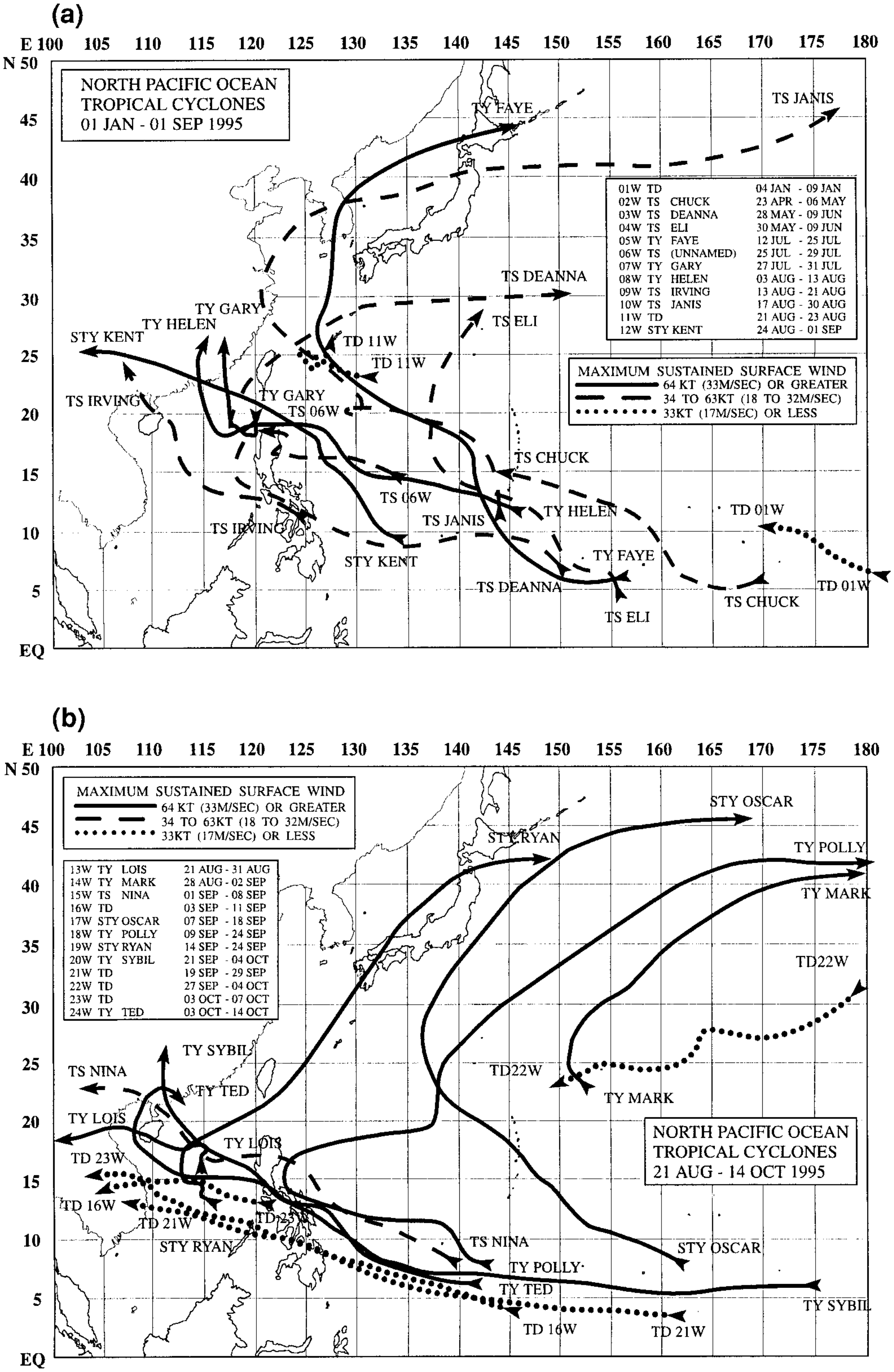

FIG. 9. Composite best tracks for (a) the WNP TCs for the period 1 January–1 September 1995; (b) 21 August–14 September 1995; and, (c) 5 October–31 December 1995.

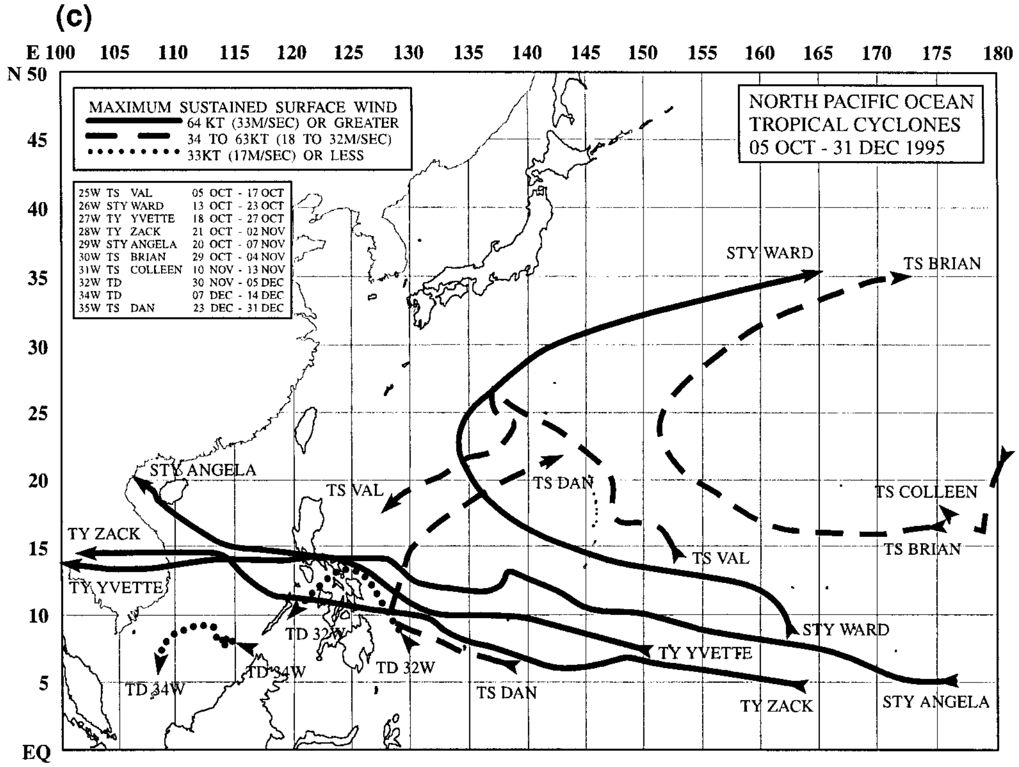

FIG. 9. (*Continued*)

briefly in the northern part of Kent's eye, observed a peak wind gust of 140 kt and a minimum sea level pressure of 928 hPa. Hourly radar images from Kaohsiung, Taiwan, showed concentric eyewalls that persisted for at least 22 h. Kent continued on a west-northwest track and made landfall in China, just east of Hong Kong. Lois became a typhoon as it was passing over the southern end of Hainan Island in the SCS and later made landfall in northern Vietnam. Lois was one of an unusually large number of TCs (eight) that formed in the SCS during 1995.

At the end of August, Mark (14W) formed at a relatively high latitude. Mark was a small TC that moved northeastward for most of its track. It did not reach peak intensity until the first day of September.

9) SEPTEMBER

September was more active than August, with a total of nine significant TCs: eight that formed during the month and one (Mark) that was still active from August. On the first day of the month, Mark was moving in excess of 20 kt (37 km h^{-1}) toward the polar front. While passing over increasingly cooler sea surface temperatures, it acquired a well-defined eye and reached a peak estimated intensity of 95 kt (49 m s^{-1}) as it tracked northeastward from 35° to 37°N.

During the first week of September, two relatively weak TCs—Nina (15W) and Tropical Depression 16W (TD 16W)—formed in a weak monsoon trough, crossed the Philippines, and entered the SCS. Nina ultimately made landfall in southern China. TD 16°W made landfall in Vietnam and survived its passage across southeast Asia and entered the Bay of Bengal, where it regenerated and became Tropical Cyclone 01B.

During mid-September, the first of two relatively active monsoon episodes during 1995 occurred. A reverse-oriented monsoon trough (Lander 1996) formed. Its axis stretching from the SCS eastward across Luzon and the Philippine Sea and then northeastward to the northeast of Guam. This episode of a reverse-oriented monsoon trough saw the simultaneous development of three TCs along its axis—Oscar (17W), Polly (18W), and Ryan (19W).

Oscar (17W) became a very large TC. It also became a very intense TC, reaching a peak intensity of 140 kt (72 m s^{-1}). Oscar posed a serious threat to Tokyo and the southeastern coast of Japan, however, it recurved enough eastward to give only a glancing blow to extreme southeastern Honshu; the eye remained offshore as it passed about 100 n mi (185 km) southeast of Tokyo. Oscar's rapid speed of translation—in excess of 40 kt (75 km h^{-1})—helped to spare Japan the full effects of the typhoon's highest winds. Nevertheless, heavy rain and high winds were responsible for loss of life and some minor damage in Japan.

Like many other TCs that form within (or move into) a reverse-oriented monsoon trough, Polly (18W) underwent unusual motion: an ''S''-shaped track. Polly reached peak intensity of 90 kt (46 m s^{-1}) before it turned to the north-northeast on the final leg of its S track. The extratropical remains of Polly, possessing a well-defined low-level circulation, moved across the international date line on 24 September.

Ryan (19W) was the first TC in JTWC's records to both form and attain super typhoon intensity within the SCS. As was also the case with Polly (18W), Ryan moved on an S-shaped track. Ryan passed through the southern islands of the Ryukyu chain, and made landfall in southwestern Japan. On 22 September, Ryan passed near the Taiwanese island of Lanyu (WMO 46762) where a peak wind gust of 166 kt (85.3 m s^{-1}) tied the strongest wind gust ever recorded in a typhoon. The other event occurred at Miyako Jima (WMO 47927) in September 1966 near the eye of Typhoon Cora.

After the reverse-oriented monsoon trough of mid-September migrated out of the Tropics, a near-equatorial trough was reestablished across Micronesia during the final week of September. Sibyl (20W) and Tropical Depression 21W (TD 21W) formed in this trough. Sibyl reached its peak intensity of 95 kt (49 m s^{-1}) as it crossed the Visayan Islands. Later, it tracked over metro Manila and entered the SCS, where it slowly weakened before making landfall east of the Luichow peninsula in southern China. The tropical disturbance that became TD 21W crossed the Philippines on 25 September, and on 28 September, as this tropical disturbance neared the coast of Vietnam, the deep convection consolidated near the low-level circulation center and it became TD 21W. The system made landfall on the coast of Vietnam and dissipated.

An unusual TC—Tropical Depression 22W (TD 22W)—formed at the end of the month and continued into October. Tropical depression 22W formed at a relatively high latitude (30°N) near the international date line. It was a very small TC—the smallest significant TC in the WNP warned on by the JTWC during 1995.

10) OCTOBER

October was a month of above normal TC activity in the WNP: eight TCs formed during the month, and two—TD 22W and Sibyl (20W)—formed during September, but were active until 4 October. The first TC that formed during October was Tropical Depression 23W (TD 23W). The tropical disturbance that became TD 23W originated over the Philippines and briefly became a tropical depression with maximum winds of 25 kt (13 m s^{-1}) as it moved westward over the SCS. Ted (24W) developed east of the Philippines in the near-equatorial trough. After moving through the islands of the central Philippines as a tropical disturbance, Ted became a typhoon in the SCS when south of Hainan Island. As Ted passed into the Gulf of Tonkin, a gust of 111 kt (55 m s^{-1}) was measured at 100 m above sea level atop an oil rig. Ted eventually dissipated over the mountains of southern China.

In the mean, during October, the axis of the monsoon trough extended across Luzon and into the Philippine Sea to the southwest of Guam. This is where it remained for most of the month with one major exception: during mid-October a large monsoon gyre formed in the Philippine Sea. Tropical Storm Val (25W) interacted with this monsoon gyre: Val orbited from the eastern side of the gyre to its northern side. Eventually, all of Val's deep convection was sheared away, and it merged with the monsoon gyre. The merged vortex drifted to the west-southwest and slowly dissipated. After the monsoon gyre dissipated in the latter half of October, the monsoon trough axis became reestablished across the Philippine Sea from Luzon to the southwest of Guam. During the latter half of October, all TCs—Ward (26W), Yvette (27W), Zack (28W), and Angela (29W)—except the TUTT-related Brian (30W), formed near, or west, of Guam.

The fourth of five supertyphoons during 1995, Ward (26W) formed as a small TC east of Guam. Moving rather quickly at 17 kt (32 km h^{-1}) toward the west, Ward passed between the islands of Rota and Saipan, or about 70 n mi (130 km) to the north of Guam, during the night of 17 October. While approaching its point of recurvature, Ward also intensified, and attained a peak intensity of 140 kt (72 m s^{-1}).

Yvette (27W) was one of seven TCs during 1995 that passed over the Philippines with an intensity of 35 kt (18 m s^{-1}) or greater. Like many other TCs during 1995, Yvette did not develop significantly until it had tracked westward to near the Philippines where it finally became a tropical storm. After crossing the Philippines, Yvette moved westward over the SCS where it reached typhoon intensity just before making landfall along the coast of Vietnam.

Originating from a tropical disturbance in the eastern Caroline Islands, Zack (28W) did not significantly intensify for nearly six days. As was the case with Sibyl (20W), Zack intensified as it crossed the Visayan Islands. But, unlike Sibyl (which weakened over the South China Sea after crossing the Philippines), Zack intensified significantly, peaking at an intensity of 120 kt (62 m s^{-1}).

Angela (29W) was the most intense typhoon of 1995, and it was the most intense typhoon to hit the Philippines since Typhoon Joan (1970). First striking southern Luzon, it moved westward and crossed the metro Manila area. More than 600 people perished in the Philippines as a result of Angela. Like many of the 1995 TCs, Angela was slow to develop, but ultimately, it became one of the most intense typhoons of the decade when it peaked at an intensity of 155 kt (80 m s^{-1}).

During the final days of October, Brian (30W) formed in direct association with a TUTT cell. Typical of such TCs, Brian was small and embedded in the easterly wind flow on the southwestern quadrant of the low-level sub-

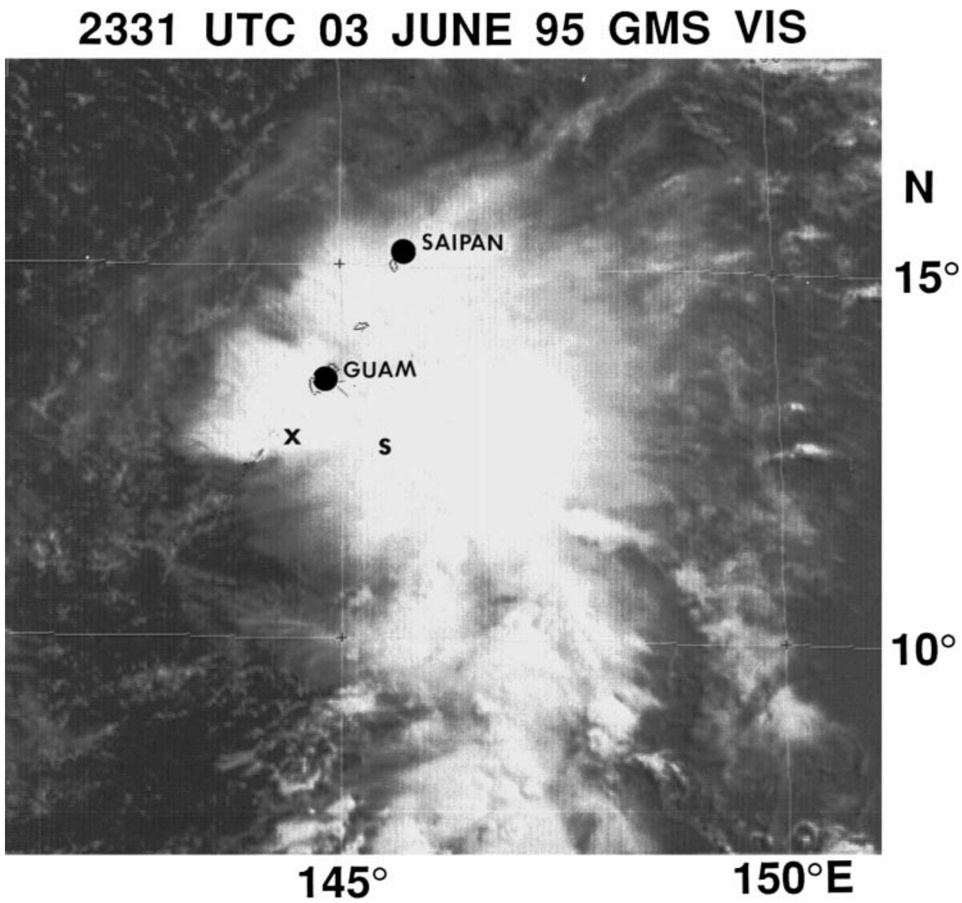

FIG. 10. Eli at minimal tropical storm intensity passes south of Guam. The ''×'' indicates low-level circulation center position as determined from NEXRAD, and ''s'' indicates satellite fix position.

tropical high. It recurved and became absorbed into the cloud band of an advancing cold front.

11) NOVEMBER

Easterly wind anomalies related to La Niña dominated the Tropics of the WNP during November and, as a consequence, November was very quiet. As November began, Brian was recurving, and only one TC—Colleen (31W)—formed during the month. On the final day of the month, a tropical disturbance that would become Tropical Depression 32W formed near the Philippines.

Colleen (31W) developed in an unusual manner for a TC in the WNP. The disturbance that became Colleen was a cutoff low that formed in the subtropics to the northwest of Hawaii—a classic ''kona'' low (Ramage 1971). Drifting toward the southwest, the kona low crossed the international date line into JTWC's AOR, where it acquired persistent central convection and became a tropical storm. Colleen was a tropical storm for only 6 h and dissipated 420 n mi (800 km) east-southeast of Wake Island.

12) DECEMBER

Three significant TCs formed in the WNP during December—Tropical Depression 32/33W, Tropical Depression 34W, and Tropical Storm Dan. The tropical disturbance that became Tropical Depression 32W (TD 32W) formed near the Philippines on the last day of November. As it drifted toward the central Philippines on 2 December, it intensified and was upgraded by the JTWC to TD 32W. Deep convection moving northward along a shear line was originally thought to be TD 32W. After this convection dissipated, a new area of persistent deep convection formed over the central Philippines and it was, at the time, upgraded to Tropical Depression 33W. Tropical Depression 33W dissipated as it moved westward toward the South China Sea. Postanalysis indicated that TD 33W was the regeneration of Tropical Depression 32W, and the two best tracks were combined as one.

On 7 December, satellite imagery and synoptic data showed that a low-level circulation center was associated with an area of persistent deep convection northwest of Borneo. Based on ship reports indicating wind

FIG. 11. NEXRAD 3-h integrated rainfall total ending at 0100 UTC 4 June. Shaded regions depicting the total rainfall over a 3-h period exhibit curved paths that imply a center about 30 nm southwest of Guam. The NEXRAD was producing mesocyclone alerts at the location marked with an "×."

speeds of 30 kt (15 m s^{-1}) near the low-level circulation center, this system was upgraded to Tropical Depression 34W (TD 34W). Wind speeds of 40 kt (21 m s^{-1}) were occurring throughout much of SCS to the north of TD 34W as a manifestation of a surge in the northeast monsoon. Tropical depression 34W formed from processes that produce TC twins during times of enhanced equatorial westerly winds (Lander 1990), and it was the Northern Hemisphere twin to Tropical Cyclone Frank (03S) in the SH. Tropical Depression 34W dissipated over water near 7°N, 109°E.

Dan (35W) was the last significant TC to occur in the WNP during 1995. Like many other TCs during 1995, Dan did not develop until it had tracked westward to near the Philippines. During December 1995, strong trade winds dominated the Tropics of the WNP. A persistent trade-wind convergence zone developed along 5°N, extending from 170°W to 140°E. Several tropical disturbances formed in the convergence zone and moved across the southern islands of Micronesia. These disturbances, coupled with the penetration of shear lines into low latitudes, produced heavier than normal rainfall across Guam and the Northern Mariana Islands. One of these disturbances became Dan. Dan reached a peak intensity of 55 kt (28 m s^{-1}), and early on 30 December, it began to accelerate toward the northeast. Moving to the northeast in excess of 30 kt (55 km h^{-1}), the last TC warning of 1995 was issued on Dan, valid at 0600 UTC 31 December, when the system became an extratropical low.

c. Some noteworthy tropical cyclones of the WNP during 1995

A comprehensive postanalysis provides insight into the behavior of a TC in a specific situation. The goal of such an analysis is to produce a more exact, definitive product from the usually vague, imprecise, and often incomplete data input. Based upon the results of the postanalysis, the JTWC compiles its final best-track database. As part of its postanalysis charter, the JTWC also generates narrative summaries (published in the

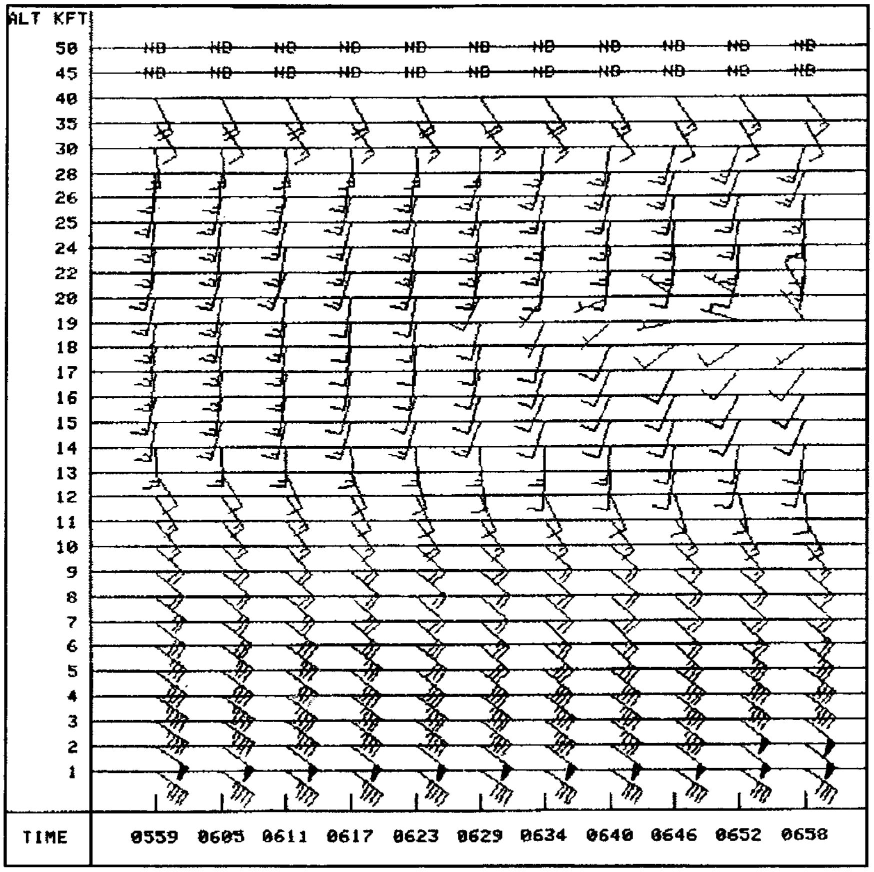

FIG. 12. NEXRAD velocity–azimuth display wind profile for the period 0559 UTC 4 June–0658 UTC 4 June shows that the maximum winds associated with Eli are located at 2000–3000 feet.

ATCR) that include the warning history, synoptic discussion, satellite imagery, and damage assessment for all significant TCs occurring in the WNP and the NIO. Due to the large number of TCs in the JTWC's AOR, narrative summaries of only seven selected WNP TCs now follow.

1) TROPICAL STORM ELI (04W)

Reason for selection: Eli came within range of Guam's NEXRAD (Next Generation Weather Radar).

On the morning of 4 June, the tropical disturbance that became Eli passed 30 n mi (55 km) south of Guam. During the day, the wind speeds on Guam increased as the sea level pressure fell. The location of the low-level circulation center as diagnosed from satellite and as determined from NEXRAD products differed by 90 n mi (170 km) (Fig. 10). Guam's NEXRAD provided crucial information that allowed for a more accurate estimate of position of the low-level circulation center. The curved paths of the integrated rainfall on the NEXRAD 3-h precipitation product (Fig. 11) implied a circulation center was located about 30 n mi south-southwest of Guam. In fact, for a few hours (centered at 0000 UTC 4 June), the NEXRAD generated alerts on mesocyclones forming near the downstream end of the primary rainband.

The NEXRAD vertical wind profiles over Guam during the afternoon of 4 June (Fig. 12) showed a peak wind velocity in the lowest levels (2000 to 3000 ft) of the troposphere. The 50-kt winds at 2000 ft were reflected in a peak wind gust to 48 kt (25 m s^{-1}) at Guam's commercial port.

2) TROPICAL STORM IRVING (09W)

Reasons for selection: Irving was very small, and microwave imagery was used to help diagnose its intensity.

The second of eight TCs to form in, or near, the SCS during 1995, Irving was very small. Isolated in an otherwise relatively cloud-free region of the SCS (Fig. 13), Irving maintained a very small CDO under which microwave imagery indicated the presence of an eye (Fig. 14).

Tropical Storm Irving was one of the smallest TCs of 1995—only Tropical Depression 22W was smaller. In fact, from the perspective of the size of Irving's sat-

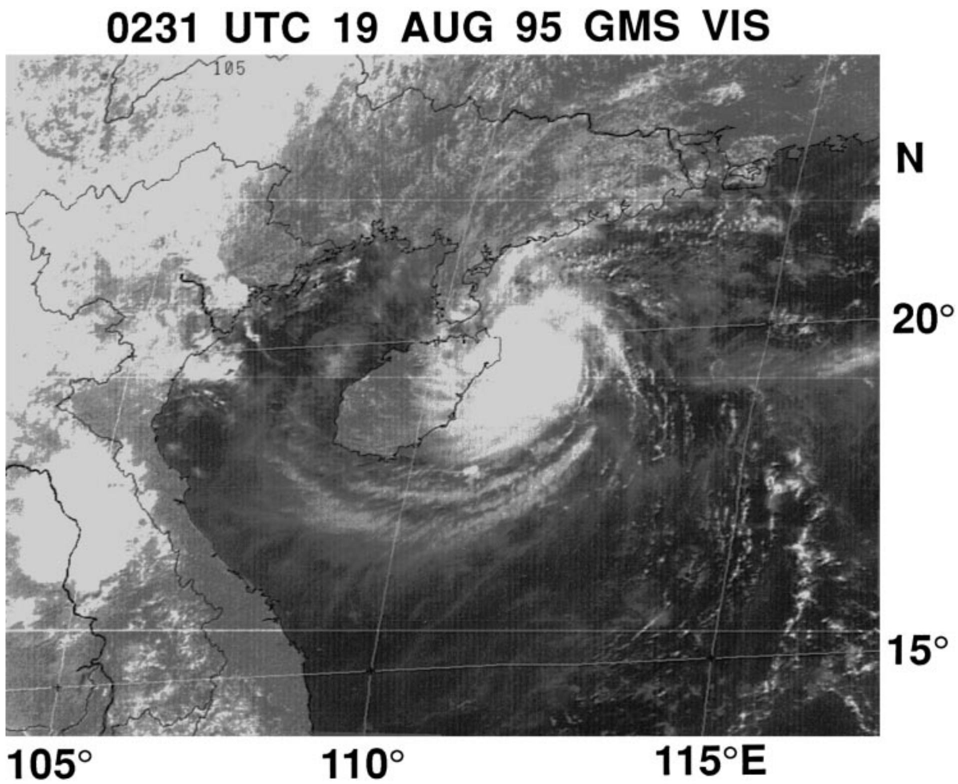

FIG. 13. Tropical Storm Irving at its peak intensity of 60 kt (31 m s^{-1}).

ellite-observed cloud shield (including the CDO and curved cirrus outflow streamers), there are few TCs in recent years that have been as small. Since 1990, only Cecil (1990), Ellie (1991), Zelda (1991), and Ofelia (1993) have been of similar size.

If it were not for satellite imagery, it is doubtful that Irving would have ever been detected. Even with detection of Irving by satellite, its intensity was difficult to diagnose. The rapid, and early, formation of Irving's CDO—and its very small size—did not lend itself well to Dvorak enhanced infrared analysis (Dvorak 1984), which requires that the intensity of a TC must have become at least 55 kt (28 m s^{-1}) 12 h before the ''embedded center'' technique can be applied. Microwave imagery showing a cirrus covered eye embedded in Irving's small CDO was helpful in supporting the peak intensity of 60 kt (31 m s^{-1}).

3) TYPHOON MARK (14W)

Reasons for selection: high latitude of formation, small size, and intensification over cool SST.

Forming at a relatively high latitude, Mark was a small TC that moved northeastward for most of its track. While moving in excess of 20 kt (37 km h^{-1}) toward the polar front, and while passing over increasingly cooler sea surface temperatures, Mark acquired a well-defined eye and reached a peak estimated intensity of 95 kt (49 m s^{-1}) as it tracked northeastward from 35° to 37°N. (Fig. 15a,b). The relatively high peak intensity attained by Mark was somewhat of a surprise, given the synoptic situation.

Relatively few TCs form in the WNP poleward of 25°N—during the 21-yr period 1970–1990 only 24 of 585 TCs (4%) that formed in the WNP first attained 25 kt (13 m s^{-1}) intensity at, or north, of 25°N. Mark first attained 25-kt intensity at 27°N. It became a tropical storm at 29°N, a typhoon at 31°N, and reached its peak intensity of 95 kt (49 m s^{-1}) at 35°N. The sea surface temperature at the point where Mark's intensity peaked was approximately 24°C (Fig. 16).

Mark was small. The diameter of its cloud shield was was about 100 n mi (185 km), and it encompassed a very small eye whose diameter fluctuated within a range from 5 n mi (9 km) to 10 n mi (18 km) on satellite imagery. As with many small TCs, the intensity forecasts were quite poor: on the first eight warnings (issued at 6-h intervals from 0000 UTC 30 August to 1800 UTC 31 August), the 24-h intensity was underforecast by anywhere from 20 to 40 kt (21 m s^{-1}); and the 48-h intensity was underforecast by as much as 65 kt (33 m s^{-1}).

4) SUPERTYPHOON OSCAR (17W)

Reasons for selection: Oscar was the largest TC of 1995, and a ''digital Dvorak'' algorithm was applied to hourly infrared imagery.

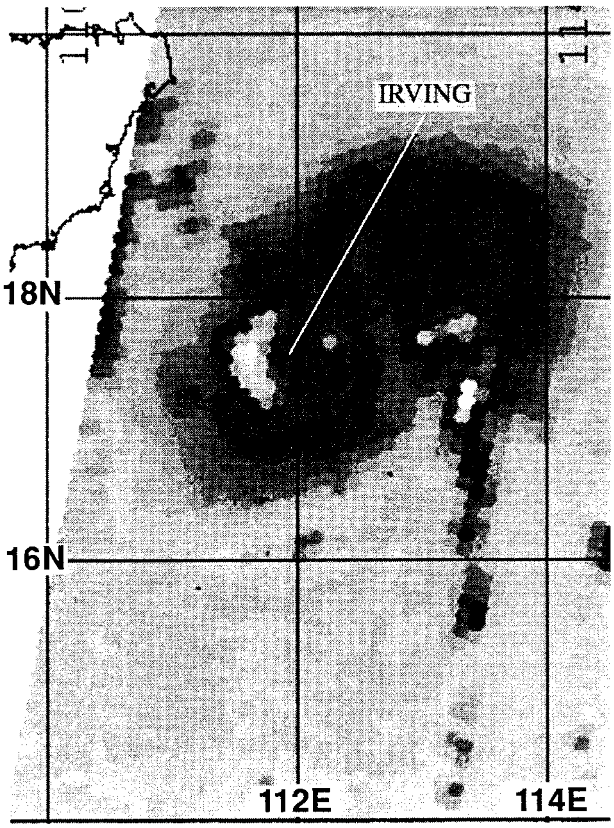

FIG. 14. A small eye is revealed by microwave imagery under the dense cirrus overcast of Irving's small CDO (2121 UTC 17 August SSM/I 85-GHz DMSP imagery).

Forming at the eastern end of a monsoon trough, which later became reverse oriented, Oscar became a large TC (Fig. 17). Oscar also became a very intense TC, reaching a peak intensity of 140 kt (72 m s^{-1}). Supertyphoon Oscar was the largest TC of 1995. Using the mean radius to the outermost closed isobar (ROCI) as a measure of Oscar's size, the system reached the threshold of the "very large" size category used by the JTWC. At its largest, the mean radius to the outermost closed isobar (ROCI) of Oscar was about 8° of great-circle arc (GCA) (Fig. 18). The large expanse of cyclonically curved low-level wind flow surrounding Oscar, the extensive cyclonically curved lines of low-level cumulus, and the deep convection surrounding Oscar extended well beyond the mean ROCI.

One of the utilities installed in the JTWC's satellite image processing equipment is an automated routine for computing Dvorak "T" numbers for TCs that possess eyes. The routine, developed by R. Zehr (1995, personal communication), adapts the rules of the Dvorak technique as subjectively applied to enhanced infrared imagery (Dvorak 1984) in order to arrive at an objective T number, or digital Dvorak T number (hereafter referred to as DD numbers). Infrared imagery is available hourly from the GMS (Geostationary Meteorological Satellite), and hourly DD numbers were calculated for several of the typhoons of 1995 (including Oscar).

The DD numbers are considered experimental, and methods for incorporating them into operational practice are being explored. In some cases, the DD numbers differ substantially from the warning intensity and also from the subjectively determined T numbers obtained from application of Dvorak's techniques. The output of the DD algorithm, when performed hourly, often undergoes rapid and large fluctuations. The fluctuations of the DD numbers may lay the groundwork for future modifications to the current methods of estimating TC intensity from satellite imagery. The discussion of the behavior of the time series of the DD numbers for Oscar, and for some of the other typhoons of 1995 [e.g., see the summaries of Ryan (19W) and Ward (26W)], is intended to highlight certain aspects of the DD time series that may prove to have important research and/or warning implications.

In Oscar's case, the DD numbers rise steadily from values in the low 5's beginning at 1630 UTC 14 September to a peak in the mid 7's within a period of a few hours either side of 1230 UTC 15 September (Fig. 19). Thereafter, the DD numbers fall quite steadily, and drop below T 4.0 after 0630 UTC on September 17. Compared with both the warning intensity, and the final best-track intensity, one can see that the DD number and the warning intensity (converted to a T number) rise in tandem. As the DD numbers began to fall, the warning intensity did not reflect this fall, but remained consistently higher. Part of the reason for this is the requirement in Dvorak's techniques that the current intensity (i.e., real-time warning intensity) be held higher than the diagnosed (or data) T number when that diagnosed T number is falling.

The time series of Oscar's DD numbers is well-behaved: they steadily rise to a peak, and then steadily fall after the peak is reached. The hour-to-hour variation is within a few tenths of a T number, and few large fluctuations are noted. Also, the warning intensity and the DD numbers are consistent. This is not always the case: for some TCs, there were large short-term variations, and the DD numbers were not consistent with the best-track intensity.

5) SUPERTYPHOON RYAN (19W)

Reasons for selection: Ryan was the first TC to form and become a supertyphoon in the SCS, and its DD time series had large fluctuations that were at considerable variance with the best-track intensity.

Ryan was the first TC on JTWC's records to both form and attain supertyphoon intensity within the SCS. Since the JTWC was established in 1959, there have been no supertyphoons—130 kt (67 m s^{-1}) or greater—in the SCS (although there have been supertyphoons in the Philippine Sea that have moved into the SCS at lesser intensities). During the period 1945–1959, before

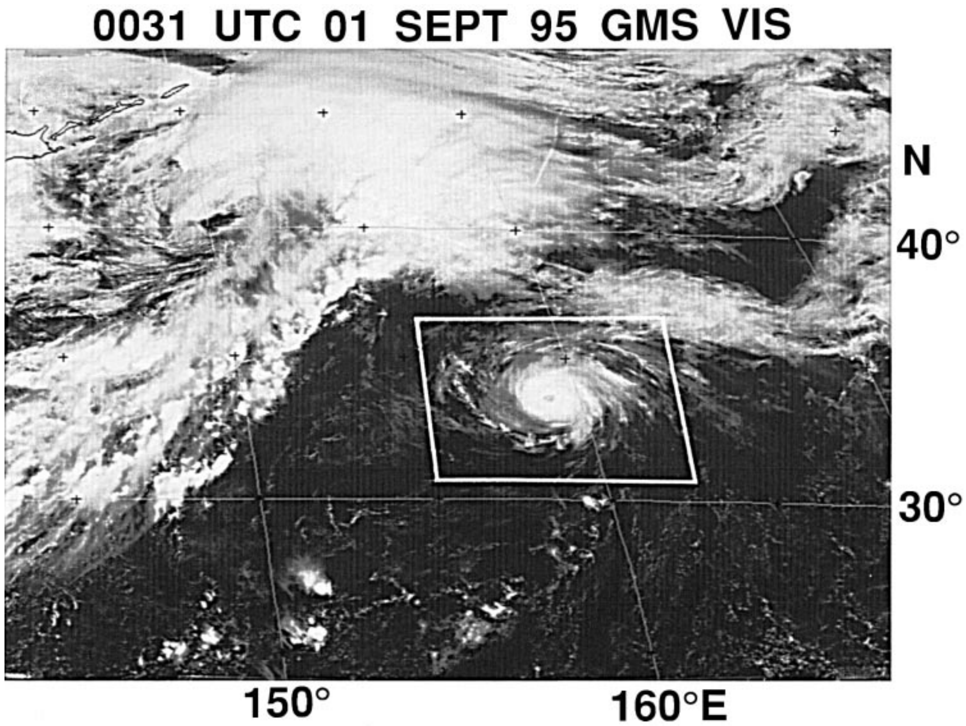

FIG. 15. Typhoon Mark (located within the white box) intensifies as it moves rapidly northeastward in the warm sector of an approaching midlatitude low pressure system (0031 UTC 1 September visible GMS imagery).

the JTWC was established, TCs in the WNP were nonetheless reconnoitered by air force and navy aircraft. During these years, two typhoons—Gloria (1952) and Betty (1953)—were reported to have attained supertyphoon intensity after crossing the Philippines and while over the SCS. In the case of these two typhoons, it is difficult to assess the reliability of the reconnaissance reports of supertyphoon intensity.

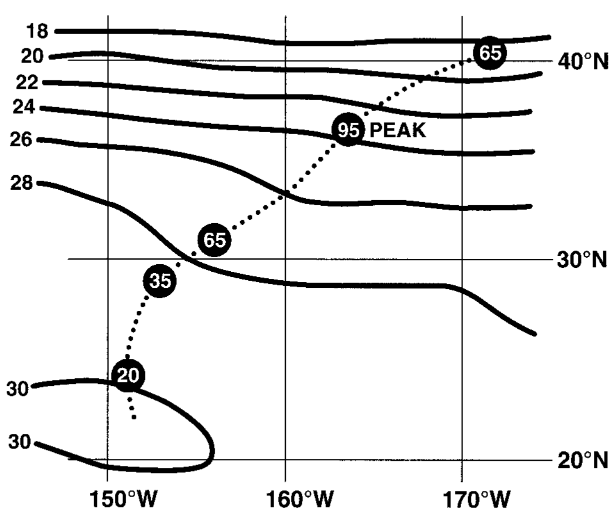

FIG. 16. Selected threshold intensities (kt) of Mark (white numbers within the black circles) along Mark's track (dotted line) superimposed on the Navy's NOGAPS sea surface temperature analysis (°C) of 2 September.

Whereas the time series of the hourly values of the DD numbers for Oscar (17W) was relatively stable, and was in good agreement with the JTWC warning intensity; the time series of Ryan's hourly DD numbers underwent some large fluctuations (Fig. 20) that were not in good agreement with the warning intensity or with the final best-track intensity. The magnitude of Ryan's DD numbers exceeded T 7.0—equivalent to an intensity of 140 kt (72 m s^{-1}) maximum sustained wind speed—twice during its life. (For maximum wind and minimum sea level pressure equivalents to Dvorak's T numbers, see Table 2). The first DD of T 7.0 occurred at 2230 UTC 19 September, and reached a peak of T 7.3 at 0230 UTC 20 September (see Fig. 21a) before falling back into values in the vicinity of T 6.0. The warning intensity at this time was 90 kt (46 m s^{-1}), and the final best-track intensity was 85 kt (44 m s^{-1}).

After the first DD peak of T 7.3, the hourly time series of the DD fell back to within a few tenths of T 6.0 for a period of about 30 h, after which the DD rose once again above T 7.0 at 1230 UTC 21 September (see Fig. 21b). The warning intensity (and final best-track intensity) for Ryan reached a peak of 130 kt (67 m s^{-1}) at this time. The warning intensity and the DD were in close agreement at this time.

That the warning intensity and best-track intensity do

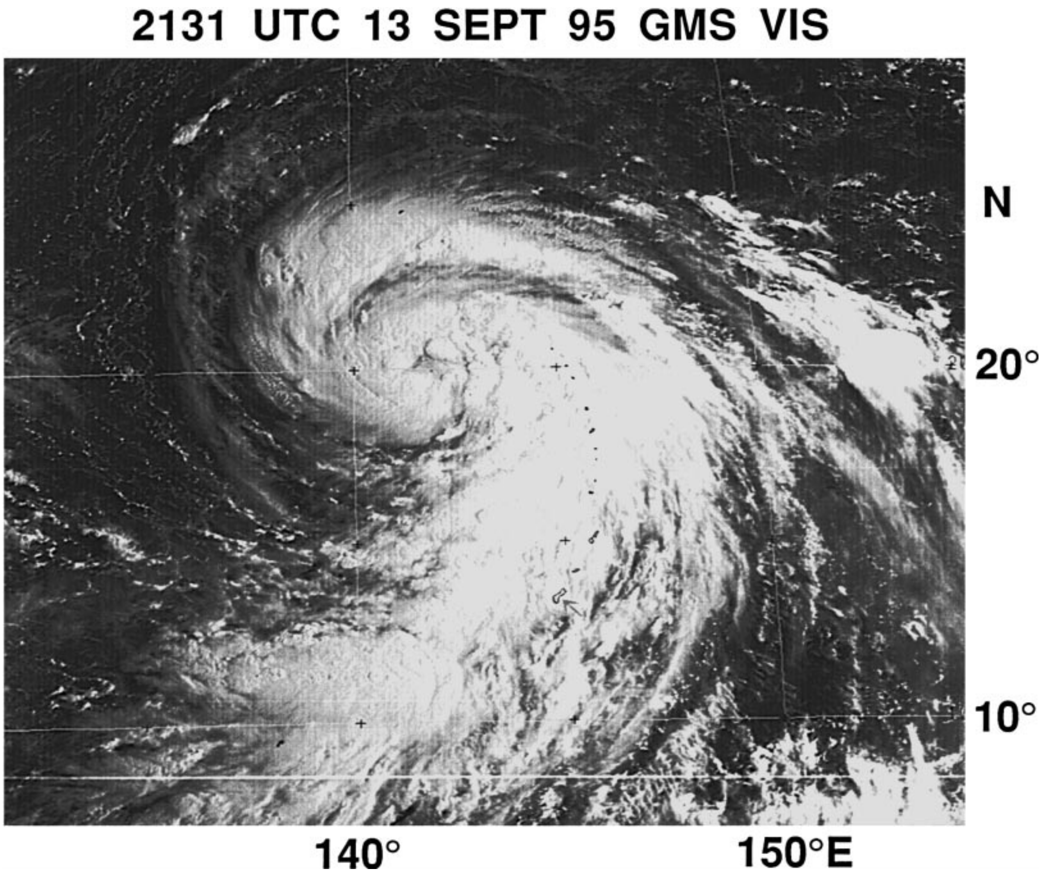

FIG. 17. As Oscar becomes a typhoon, its cloud system covers a large area of the Pacific near the Mariana Island chain. (2131 UTC 13 September visible GMS imagery.)

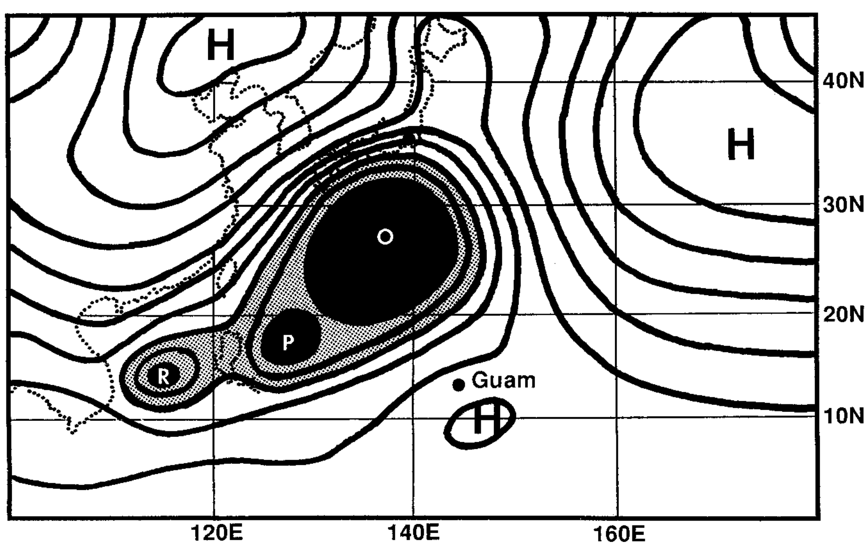

FIG. 18. Sea level pressure (SLP) analysis over the WNP at 0000 UTC 16 September. Three TCs—Oscar (O), Polly (18W) (P), and Ryan (19W) (R)—formed simultaneously along a reverse-oriented monsoon trough. Oscar's large size is indicated by its large average radius of outermost closed isobar, which has a value of approximately 500 n mi. Solid lines are isobars at 2-hPa intervals. The shaded region shows where SLP is lower than 1006 hPa, the black areas are below 1002 hPa. The 1002-hPa isobar is Oscar's outermost closed isobar.

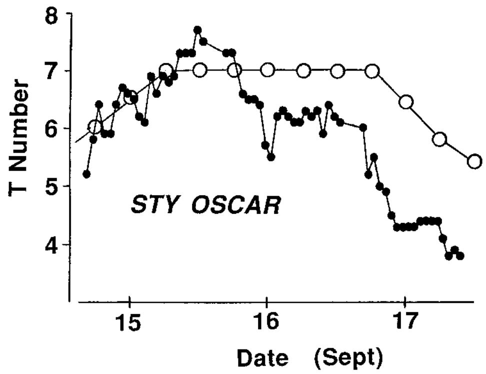

FIG. 19. The hourly time series of the DD number obtained for Oscar during the period 1630 UTC 14 September through 0930 UTC 17 September (black dots) versus the final best-track warning intensity converted to T numbers (open circles).

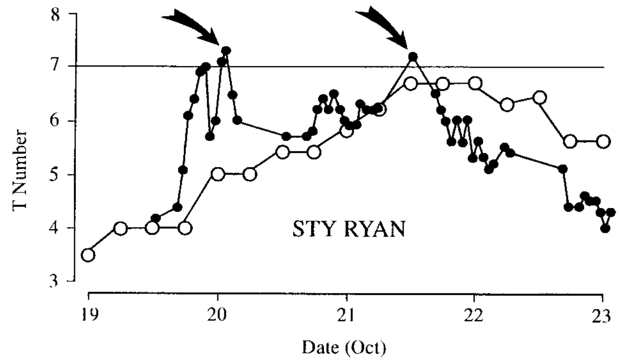

FIG. 20. The hourly time series of the DD numbers for Ryan (solid circles) for the period 19–23 September shows large fluctuations. The final best-track intensity (open circles) converted to T numbers for the period 19–23 September shows large discrepancies with the DD numbers. Arrows indicate the two instances where the DD numbers exceeded T 7.0.

not reflect the first rise of the DD to T 7.0 has several explanations. For one, the magnitude of the rise of 2.6 T numbers in 5 h (from T 4.4 to T 7.0) exceeds the constraints allowed by the Dvorak technique. For another, the final best-track data (i.e., the intensity and position at 6-h intervals) is intentionally smoothed with respect to the erratic fluctuations from fix to fix. Lastly, the DD algorithm is, as yet, experimental, and its output has little influence in the outcome of the final best-track.

6) SUPERTYPHOON WARD (25W)

Reasons for selection: Ward passed within range of Guam's NEXRAD, and its DD time series exhibited large fluctuations.

During the night of 17 October, Ward passed between the islands of Rota and Saipan, or about 70 n mi (130 km) to the north of Guam. This placed the small circulation of the intensifying Ward well within the range of Guam's NEXRAD. While within the 124-n mi range of the NEXRAD velocity measurements, Ward moved toward the west-northwest at an average translational speed of 17 kt (32 km h^{-1}) and intensified from 45 to 65 kt (23–33 m s^{-1}). One aspect of Ward's structure that was well depicted by the NEXRAD was the nature of the wind asymmetry. The wind asymmetry between the north side and the south side of Ward appeared to be primarily a result of Ward's translation speed. The effect of the translation was almost fully represented. At a translation speed of 17 kt, one would expect the difference in the wind speed between the north side and the south side of Ward to be twice the speed of translation, or approximately 35 kt. When Ward came within the Doppler velocity range, approximately 120 n mi (220 km) to the east-northeast of Guam, a maximum inbound wind of 50 kt was present on the north side at the lowest beam altitude of 16 000 ft. On the south side of Ward, the maximum outbound wind was 17 kt (also at 16 000 ft). The differential between the inbound and outbound wind was thus 33 kt, or very nearly what would be expected from a full accounting of the speed of translation. Later, as Ward moved due north of the NEXRAD (and thereby placing the asymmetry introduced by the speed of translation perpendicular to the radar), the maximum inbound and outbound velocities became nearly equal at about 65 kt each way, and both at the lowest beam altitude of 7000 ft.

Ward was a small TC as it passed to the north of Guam. When due north of Guam, the distance between the maximum inbound and outbound winds was only 12 n mi (22 km) at 7000 ft. The diameter of gale-force winds was approximately 40 n mi (75 km) at 7000 ft. The speed of the westerly winds on Guam when Ward passed only 70 n mi (130 km) to the north was only 10 kt. The subsequent growth in size and the large increase of the intensity of this small vortex was a remarkable structural change.

Ward was another of the year's TCs for which hourly

TABLE 2. Maximum sustained 1-min wind as a function of Dvorak T number.

T number	Wind speed—kt	(m s^{-1})	Min SLP (Pacific)
0.0	<25	<(13)	—
0.5	25	(13)	—
1.0	25	(13)	—
1.5	25	(13)	—
2.0	30	(15)	1000
2.5	35	(18)	997
3.0	45	(23)	991
3.5	55	(28)	984
4.0	65	(33)	976
4.5	77	(40)	966
5.0	90	(46)	954
5.5	102	(53)	941
6.0	115	(59)	927
6.5	127	(65)	914
7.0	140	(72)	898
7.5	155	(80)	879
8.0	170	(87)	858

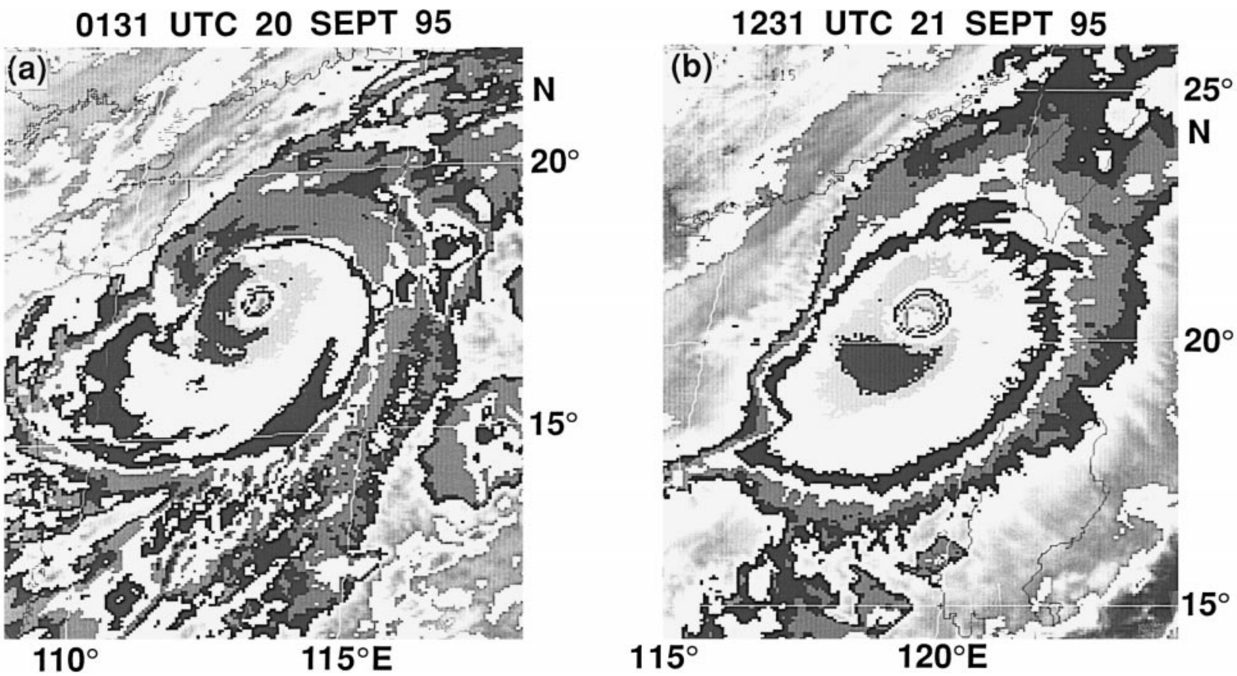

FIG. 21. (a) Ryan reaches a DD number of T 7.3 (0130 UTC 20 September enhanced infrared GMS imagery). (b) Ryan's DD number once again is greater than T 7.0 (1230 UTC 21 September enhanced infrared GMS imagery).

values of the digital Dvorak (DD) numbers were tabulated during much of its life. The time series of Ward's DD numbers (Fig. 22) indicates two peaks of intensity near T 7.0 (equivalent to 140 kt): one at approximately 1200 UTC 18 October and the other 24 h later at 1200 UTC 19 October. Between these two peaks, the DD indicated that the intensity fell as low as T 4.0 (minimal typhoon intensity) at about 0000 UTC 19 October. These two intensity peaks are closely related to the evolution of Ward's eye. After first becoming a typhoon, Ward's eye was extremely small (as seen by NEXRAD and later as it appeared on visible satellite imagery). After attaining its first intensity peak at 1200 UTC with a very small eye (Fig. 23a), the eye clouded over (resulting in lower intensity estimates) and then reappeared at a larger size when it attained its second peak intensity at 1200 UTC 19 October (Fig. 23b).

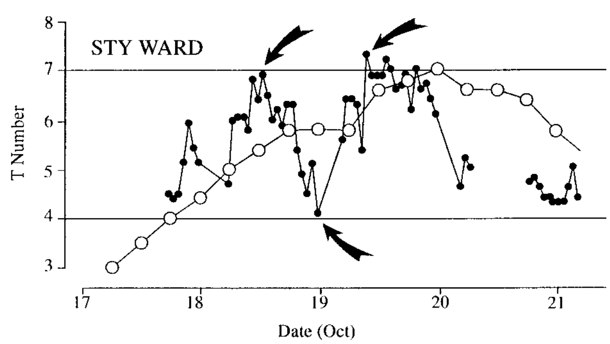

FIG. 22. A time series of Ward's hourly DD numbers (black dots). Also shown is the warning intensity (converted to a T number) (open circles). Arrows indicate two peaks and an intervening minimum in the DD time series.

Similar to the case with Ryan (19W), the warning intensity and the final best-track intensity do not reflect the first peak of the DD (i.e., DD = 140 kt; final best-track—100 kt). As the DD rose to its second peak, the warning and final best-track intensity rose to match it (i.e., DD = 140 kt; final best-track intensity—140 kt). Once again, the DD has revealed extremely large and rapid fluctuations of intensity that were not reflected in the warning intensity or the final best-track intensity. In the absence of ground-truth measurements, it is not possible to know in fine detail how Ward's intensity changed. If the DD truly represented Ward's intensity, there are two sobering implications: 1) an extremely rapid increase of intensity occurred that was not reflected in the warning, and 2) the best-track database, having had these rapid fluctuations removed, cannot be used to study the processes governing what may prove to be real intensity fluctuations of the magnitude indicated by the DD.

7) SUPERTYPHOON ANGELA (29W)

Reasons for selection: Angela was the most intense TC of 1995, it underwent explosive deepening, and it devastated portions of the Philippines.

Angela was the most intense typhoon to hit the Philippines since Typhoon Joan (1970). First striking southern Luzon, it moved westward and crossed the metro Manila area. More than 600 people perished in the Phil-

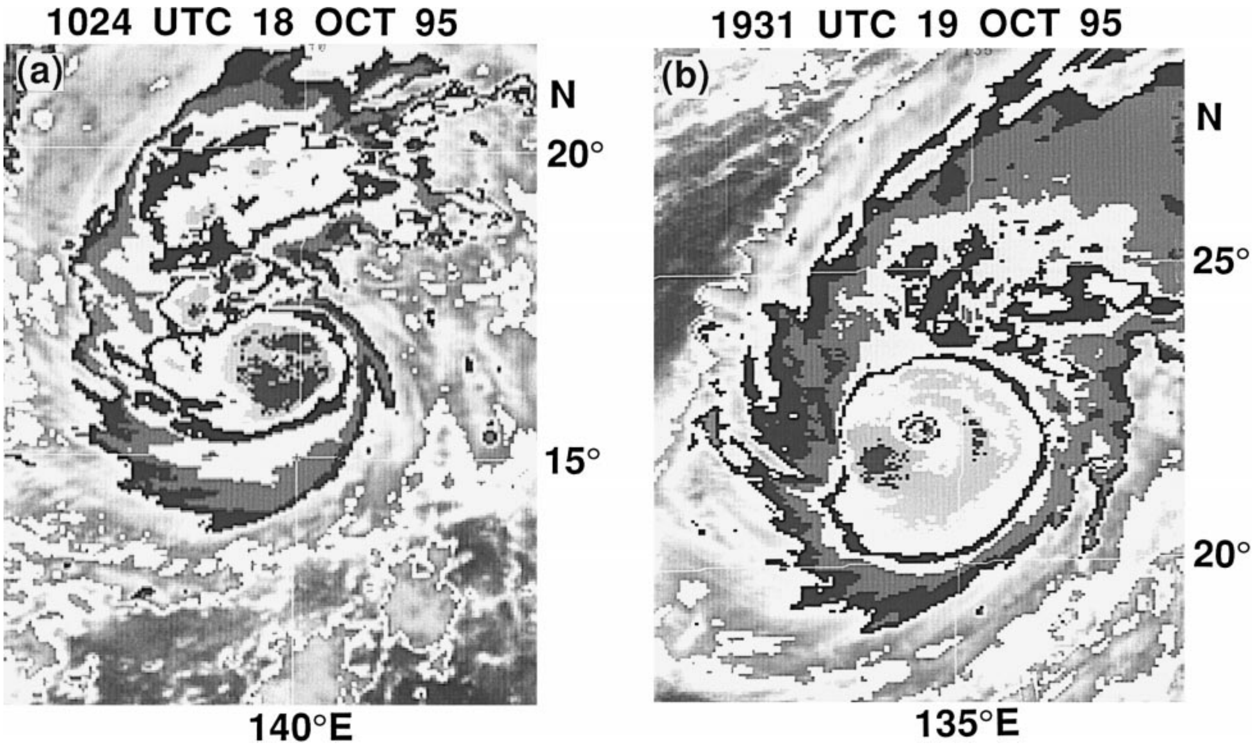

FIG. 23. (a) Ward possesses a very small eye at the time of the first peak on the DD time series (1031 UTC 18 October enhanced infrared GMS imagery). (b) Ward (its DD again near T 7.0) at peak warning intensity of 140 kt (72 m s $^{-1}$) (1931 UTC 19 October enhanced infrared GMS imagery).

ippines as a result of Angela. Angela moved westward in tandem with Typhoon Zack (28W) for nearly 4000 n mi (7400 km) across the WNP. Like many of the 1995 TCs, Angela was slow to develop, but ultimately, it became one of the most intense typhoons of the decade, peaking at an intensity of 155 kt (80 m s^{-1}) (Fig. 24).

On 31 October, after Angela's intensity had reached 90 kt (46 m s^{-1}), it began to rapidly intensify (Holliday and Thompson 1979). Eighteen hours later, Angela's maximum sustained wind had increased to 155 kt. The equivalent pressure fall over this 18-h period was 71 hPa, and the average rate of fall was 3.94 hPa h^{-1}. This meets the criterion for a special case of rapid intensification called explosive deepening (Dunnavan 1981) in which the pressure fall must exceed 2.5 hPa h^{-1} for at least 12 h.

Shortly after reaching peak intensity, Angela moved about 15 n mi (28 km) north of the Catanduenas Island radar site (WMO 98446) and 40 n mi (75 km) north of Virac, Catanduenas Island (WMO 98447). The radar site recorded gusts to 140 kt (72 m s^{-1}) and Virac had gusts to 111 kt (57 m s^{-1}). Since the radar site appeared to be in the southern eyewall, and the translation speed of Angela was toward the west at 10 kt (19 km h^{-1}), a reasonable estimation of Angela's intensity when it passed to the north of Catanduenas at 1200 UTC 2 November (taking full account of the speed of translation and using a gust factor of 1.2) is 135 kt sustained 1-min wind with gusts to 160 kt (69G82 m s^{-1}). After its close passage to Catanduenas, Angela moved westward, and at 1900 UTC 2 November the center of Angela's eye passed over Daet (WMO 98440), where the sea level pressure fell to a minimum of 926 hPa and a peak wind gust of 135 kt (69 m s^{-1}) was recorded.

In the metro Manila area, wind and pressure measurements indicate that Angela's sustained winds had weakened to 80–90 kt (41–46 m s^{-1}). The center of Angela appears to have passed near or over the Ninoy Aquino International Airport in Manila (WMO 98429) where a minimum sea level pressure of 975.6 mb was recorded at 0230 UTC 3 November; the center of Angela also appears to have passed near or over Cubi Point (WMO 98426) where a minimum sea level pressure of 976.3 mb was recorded at 0330 UTC that same day.

Angela caused considerable death, destruction, and agricultural losses in the Philippines. More than 600 people perished with and additional 100 reported missing. Over 96 000 homes were destroyed, and an estimated $70 million (U.S.) in damage was inflicted on roads and bridges. Hardest hit was the northern Bicol region of southern Luzon (located approximately 185–280 km southeast of Manila). Catanduenas Island and the metro Manila area were also hard hit. There were at least 121 deaths in Calauag, Bicol, primarily from storm surge and a river that flooded when a dam burst. More than 100 perished in the neighboring village of

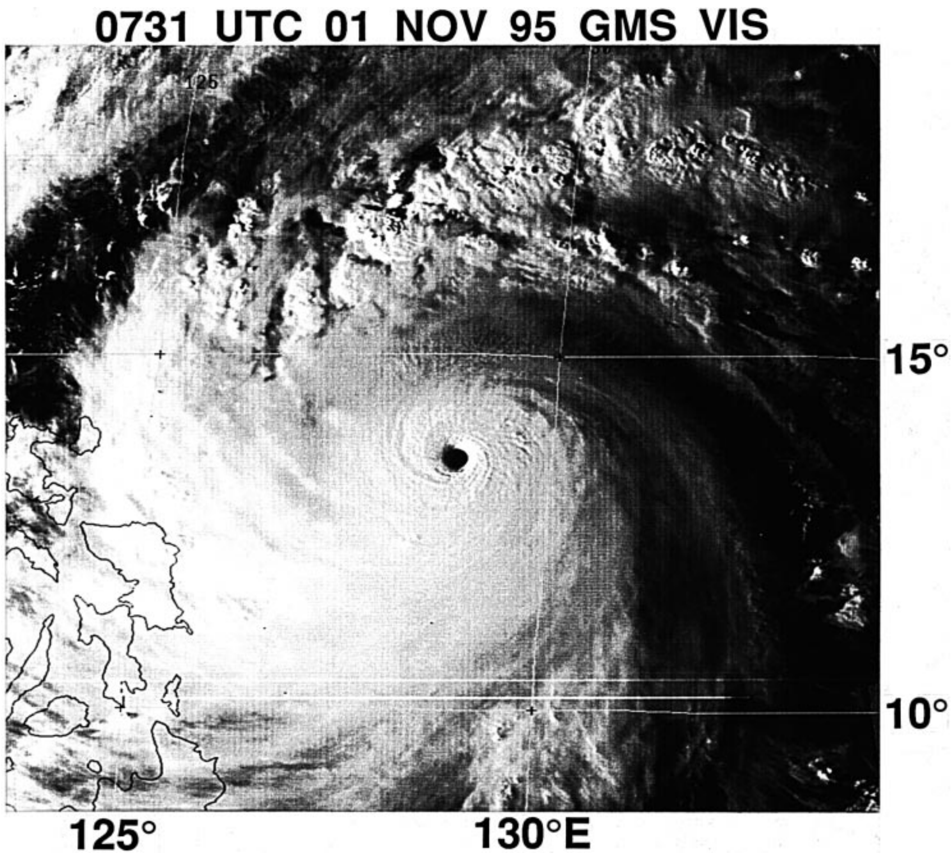

FIG. 24. Angela at peak intensity of 155 kt (80 m s^{-1}) (0731 UTC 1 November visible GMS imagery).

Paracale, primarily from mudslides. Damage to agriculture exceeded $18 million (U.S.). Electrical power was lost by one-third of the country.

3. North Indian Ocean annual summary (January–December 1995)

The JTWC statistics for the NIO are provided for reference. The time series of the annual numbers of TCs in the various ocean basins (and possible modifications to the regional and global TC distribution by climate change) have become a high-profile topic of scientific and popular interest (e.g., see Lighthill et al. 1994). In this context, it is important to note that there are significant differences between the JTWC annual number of TCs and the annual number of TCs reported by the WMO in the NIO (Table 3).

Tropical cyclones in the NIO (especially in the Bay of Bengal) have been some of the deadliest in history. In terms of storm surge, the Bay of Bengal is the most dangerous TC basin in the world. Particularly sensitive is the low-lying Ganges River delta region of Bangladesh. One of the world's greatest TC-related disasters occurred in 1970 when 300 000 lives were lost when a powerful TC made landfall there. A similar TC struck the coastal regions of Bangladesh during April 1991 and devastated the coastal city of Chittagong with winds in excess of 130 kt (67 m s^{-1}) and a 20-ft (6 m) storm surge. The official death toll of the 1991 TC was estimated at 138 000 and the damage at $1.5 billion (U.S.).

The year of 1995 included four numbered TCs in the NIO (Table 4). Two of these—TC 03B and TC 04B—exceeded typhoon intensity, and the other two—TC 01B and TC 02A—reached peak intensities of 45 and 55 kt, respectively (Table 4). Only one significant TC occurred in the Arabian Sea, and three significant TCs occurred in the Bay of Bengal. Three of the four significant TCs in the NIO during 1995 formed in the monsoon trough. Tropical cyclone 01B can be traced to the remnants of Tropical Depression 16W, which, after making landfall in Vietnam, passed across southeast Asia and regenerated in the Bay of Bengal.

The NIO is a marginal basin with a long-term annual average of five significant TCs, ranging from a high of 13 TCs during 1992 to a low of 2 TCs in 1980 and 1993. The calendar-year total of four significant TCs in the NIO during 1995 was one below the long-term average.

The NIO has one of the world's most unusual annual distributions of TCs: of the mean annual total of five, approximately two occur in the spring and three occur in the fall (there is an unusual midsummer minimum

TABLE 3. Comparison of JTWC TC totals vs WMO totals for comparable years (dashed lines indicate data not available).

Year	1969	1970	1971	1972	1973	1974	1975	1976	1977	1978	1979	1980	1981	1982	1983	1984	1985	1986	1987	1988	1989	1990	1991	1992	1993	1994	1995
JTWC (SH)	—	—	—	—	—	—	—	—	—	—	—	—	24	25	25	30	35	33	28	21	28	29	22	30	27	30	22
WMO (SH)	19	24	29	30	31	30	24	27	28	30	24	30	32	24	22	25	26	28	25	22	28	21	17	24	23	27	19
JTWC (NIO)							6	5	5	4	7	2	3	5	3	4	6	3	8	5	3	4	4	13	2	5	4
WMO (NIO)							7	10	6	6	5	3	6	5	3	3	7	1	5	3	3		—	—	—	—	—

when the monsoon trough has moved to its northernmost position, mostly over land). During 1995, there were no significant TCs in the NIO during the spring. All four of the 1995 significant TCs in the NIO occurred in the two-month period September 16–November 18.

4. Southern Hemisphere annual summary (July 1994–June 1995)

The JTWC statistics for the SH are provided for reference. The time series of the annual numbers of TCs in the various ocean basins (and possible modifications to the regional and global TC distribution by climate change) has become a high-profile topic of scientific and popular interest (e.g., see Lighthill et al. 1994). In this context, it is important to note that there are significant differences between the JTWC SH statistics and the TC statistics provided by the RSMC's (e.g., the Australian Bureau of Meteorology, Fiji, and La Réunion) in these regions (Table 3).

During the period July 1994–June 1995, there were 22 significant TCs in the SH including 12 of hurricane intensity, seven tropical storms, and two tropical depressions (Table 5). The annual total of 22 significant TCs in the SH was six below the long-term (14-yr) JTWC average, and was nearly a record low: only one year, 1988, had fewer, with only 21 significant TCs.

With respect to interannual changes in the genesis locations within the WNP and the SH, there are well-known and strong associations with ENSO. For the WNP there is a pronounced eastward shift of the mean genesis location during El Niño years, and a pronounced westward shift of the mean genesis location during La Niña years (Chan 1985; Dong 1988; Lander 1994b). A similarly pronounced ENSO-related shift in the annual-mean location of TC genesis has been shown to exist in the South Pacific (SPac) (e.g., Basher and Zheng 1995). During El Niño years, TC formation in the SPac is drawn eastward and equatorward. In the extreme case of the El Niño of 1982–83, TC genesis occurred as far east as the Marquesas Islands (10°S, 140°W). During La Niña years, TC formation in the SPac tends to occur further westward and southward (i.e., closer to Australia). During 1995, there were two tropical storms, one hurricane, and one tropical depression (TD) east of 165°E in the SH; consistent with the demise of the warm phase of ENSO During 1995, the two tropical storms and the hurricane occurred at the end of 1994 when low-latitude low-level wind anomalies were still westerly in that region. The TD was short-lived and formed near the international date line during March. The remainder of the SH TC activity during 1995 was weighted toward the South Indian Ocean (west of 105°E), where 11 (50%) of the TCs occurred; and in the Australian region (between 105° and 165°E) where 7 (33%) occurred.

TABLE 4. North Indian Ocean 1995 tropical cyclone statistics.

Tropical cyclone number[a]	Name[a]	Class[b]	Dates[c]	Maximum 1-min wind (m s^{-1})	Minimum SLP (mb)
01B	—	TS	16–17 Sep	23	991
02A	—	TS	12–17 Oct	26	987
03B	—	TY	7–9 Nov	36	972
04B	—	TY	21–25 Nov	54	938

[a] The numbers are according to the JTWC: A = Arabian Sea, B = Bay of Bengal. Tropical cyclones in the North Indian Ocean are not named by the New Delhi RSMC.

[b] TD: tropical depression, wind speed less than 17 m s^{-1}. TS: tropical storm, wind speed 17–32 m s^{-1}. TY: typhoon, wind speed 33 m s^{-1} or higher. STY: supertyphoon, subset of the hurricane category with wind speed greater than 66 m s^{-1}.

[c] Dates begin at 0000 UTC and include only the period of warning.

5. Concluding remarks

Historically, the JTWC has provided a summary of the TCs within its AOR in its ATCR (e.g., JTWC 1994). The ATCR has a limited distribution, and there have been requests that the JTWC provide an annual summary in *Monthly Weather Review* (*MWR*) similar to the Atlantic and eastern North Pacific TC summaries that the NHC publishes therein. This is the first year that the JTWC annual TC summary has been adapted for publication in *MWR*, and we hope to continue to provide it.

The first year for which this adaptation has been made is for the summary of the TCs of 1995 (a year conspicuous for an abundance of Atlantic TCs). Overall, 1995 was a relatively quiet year in the Eastern Hemisphere: the 22 tropical cyclones of the Southern Hemisphere were only one shy of the record low of 21, and for the first time since 1988 the number of tropical storms and typhoons in the western North Pacific was below normal.

During 1995, a prolonged period of the warm phase of the ENSO came to an end. By July of 1995, the SST along the equator in the central and eastern Pacific had become colder than normal, the SOI had risen to near zero, and low-level easterly wind anomalies replaced westerly wind anomalies in the low latitudes of the

TABLE 5. Southern Hemisphere 1995[a] tropical cyclone statistics.

Tropical cyclone number[b]	Name[b]	Class[c]	Dates[d]	Maximum 1-min wind (m s^{-1})	Minimum SLP (mb)
01P	Vania	TS	13–17 Nov 94	28	984
02S	Albertine	H	24 Nov–1 Dec	59	927
03S	Annette	H	15–19 Dec	57	933
04P	—	TS	15–17 Dec	18	997
05P	William	H	31 Dec 94–3 Jan 95	54	976
06S	Bentha	TS	3–6 Jan	28	984
07S	Christelle	TS	6–9 Jan	21	994
08S	Dorina	H	20–29 Jan	51	944
09S	Fodah	TS	24–26 Jan	23	990
10S	Gail	H	5–11 Feb	39	967
11S	Heida	TS	5–7 Feb	21	994
12S	Bobby	H	21–26 Feb	57	933
13S	Ingrid	H	24 Feb–1 Mar	51	944
14P	Violet	H	3–7 Mar	39	967
15P	Warren	TS	5–6 Mar	28	984
16S	Josta	H	7–12 Mar	33	976
17S	Kylie	H	7–14 Mar	44	958
18P	—	TD	16–17 Mar	15	1000
19S	Marlene	H	30 Mar–10 Apr 24	64	916
20S	—	TD	3–5 Apr	13	1002
21S	Chloe	H	5–8 Apr	64	964
22S	Agnes	H	17–22 Apr	57	933

[a] The Southern Hemisphere statistics for 1995 are compiled by the JTWC for the period July 1994–June 1995.

[b] The numbers are according to the JTWC: P = South Pacific, S = South Indian Ocean. The names are provided by the responsible WMO-designated RSMC (e.g., La Reunion, Perth, Darwin, Brisbane, Fiji, Port Moresby).

[c] TD: tropical depression, wind speed less than 17 m s^{-1}. TS: tropical storm, wind speed 17–32 m s^{-1}. H: hurricane, wind speed 33 m s^{-1} or higher. SH: superhurricane, subset of the hurricane category with wind speed greater than 66 m s^{-1}.

[d] Dates begin at 0000 UTC and include only the period of warning.

WNP. In some respects (e.g., the cooling of the equatorial sea surface, and the anomalously strong low-level easterly winds in the low latitudes of the WNP), the climatic anomalies of the Pacific basin during most of 1995 were consistent with those expected during a cold phase of ENSO, sometimes referred to as La Niña or El Viejo. Consistent with the onset of La Niña climatic anomalies, 1995 was a year with a weak monsoon, a below average number of typhoons, many weak and poorly defined TCs, and a westward shift of the formation region of TCs in the WNP.

The time series of the annual numbers of TCs in the various ocean basins (and possible modifications to the regional and global TC distribution by climate change) has become a high-profile topic of scientific and popular interest (e.g., see Lighthill et al. 1994). In this context, it is important to note that there are differences between the JTWC statistics and the TC statistics (e.g., annual number of TCs, and their tracks and intensities) provided by the other RSMC's within the JTWC's AOR. The JTWC TC statistics are therefore an important geophysical data record.

Acknowledgments. Support for the preparation and publication of this paper was provided by the Office of Naval Research through Grant N00014-96-1-0744. The support of the personnel at the Joint Typhoon Warning Center in allowing us access to their satellite imagery and other meteorological data is greatly appreciated. A special thanks is owed to Andy Grant for his work on the graphics. Additional technical support for this paper was provided by Mr. Charles Guard. Thanks must also go to the anonymous reviewers whose suggestions were used to improve the text.

REFERENCES

Basher, R. E., and X. Zheng, 1995: Tropical cyclones in the southwest Pacific: Spatial patterns and relationships to Southern Oscillation and sea surface temperature. *J. Climate,* **8,** 1249–1260.

Chan, J. C. L., 1985: Tropical cyclone activity in the northwest Pacific in relation to the El Niño/Southern Oscillation phenomenon. *Mon. Wea. Rev.,* **113,** 599–606.

Climate Prediction Center (CPC), 1995: Monthly 850 mb and 200 mb wind anomalies. Climate Diagnostics Bulletin, U.S. Climate Prediction Center, Dept. of Commerce, Washington, D.C.

Dong, K., 1988: El Niño and tropical cyclone frequency in the Australian region and the northwest Pacific. *Aust. Meteor. Mag.,* **36,** 219–255.

Dunnavan, G. M., 1981: Forecasting intense tropical cyclones using 700 mb equivalent potential temperature and central sea-level pressure. NOCC/JTWC Tech. Note 81-1, 12 pp.

Dvorak, V. F., 1984: Tropical cyclone intensity analysis using satellite data. NOAA Tech. Rep. NESDIS 11, 46 pp. [Available from NOAA NESDIS, 5200 Auth Road, Camp Springs, MD 20746.]

Guard, C. P., L. E. Carr, F. H. Wells, R. A. Jeffries, N. D. Gural, and D. K. Edson, 1992: Joint Typhoon Warning Center and the challenges of multibasin tropical cyclone forecasting. *Wea. Forecasting,* **7,** 328–352.

Holliday, C. R., and A. H. Thompson, 1979: Climatological characteristics of rapidly intensifying typhoons. *Mon. Wea. Rev.,* **107,** 1022–1034.

JTWC, 1994: Annual tropical cyclone report. Joint Typhoon Warning Center, 289 pp. [NTIS AD A301618.]

Lander, M. A., 1990: Evolution of the cloud pattern during the formation of tropical cyclone twins symmetrical with respect to the equator. *Mon. Wea. Rev.,* **118,** 1194–1202.

——, 1994a: An exploration of the relationships between tropical storm formation in the western North Pacific and ENSO. *Mon. Wea. Rev.,* **122,** 636–651.

——, 1994b: Description of a monsoon gyre and its effects on the tropical cyclones in the western North Pacific during August 1991. *Wea. Forecasting,* **9,** 640–654.

——, 1996: Specific tropical cyclone track types and unusual tropical cyclone motions associated with a reverse-oriented monsoon trough in the western North Pacific. *Wea. Forecasting,* **11,** 170–186.

Lighthill, J., G. J. Holland, W. M. Gray, C. Landsea, G. Craig, J. Evans, Y. Kurihara, and C. P. Guard, 1994: Global climate change and tropical cyclones. *Bull. Amer. Meteor. Soc.,* **75,** 2147–2157.

Ramage, C. S., 1971: *Monsoon Meteorology.* Academic Press, 296 pp.

Simpson, R. H., 1974: The hurricane disaster potential scale. *Weatherwise,* **27,** 169–186.